Synthesis of Enantiomerically Pure 1,5,5-Trideuterated *cis*- and *trans*-2,4-Dioxa-3-phosphadecalins. ^{31}P-NMR Evidence of Covalent-Bond Formation and the Stereochemical Implications in the Course of the Inhibition of δ-Chymotrypsin

by **Markus J. Stöckli** and **Peter Rüedi***

Organisch-chemisches Institut der Universität Zürich, Winterthurerstrasse 190, CH-8057 Zürich (phone: +41 44 635 42 41)

The irreversible inhibition of δ-chymotrypsin with the enantiomerically pure, P(3)-axially and P(3)-equatorially X-substituted *cis*- and *trans*-configurated 2,4-dioxa-3-phospha(1,5,5-$^2H_3$)bicyclo[4.4.0]-decane 3-oxides (X = F, 2,4-dinitrophenoxy) was monitored by ^{31}P-NMR spectroscopy. ^{1}H-Correlated ^{31}P{^{2}H}-NMR spectra enabled the direct observation of the vicinal coupling (^3J) between the P-atom of the inhibitor and the CH_2O moiety of Ser^{195} (= 'Ser^{195}'(CH_2O)), thus establishing the covalent nature of the 'Ser^{195}'(CH_2O-P) bond in the inhibited enzyme. The stereochemical course of the phosphorylation is dependent on the structure of the inhibitor, and neat inversion, both inversion and retention, as well as neat retention of the configuration at the P-atom was found.

1. Introduction. – Earlier ^{31}P-NMR spectroscopic investigations on the irreversible inhibition of δ-chymotrypsin with the optically active, P(3)-axially and P(3)-equatorially substituted *cis*- and *trans*-configurated 3-(2,4-dinitrophenoxy)-2,4-dioxa-3-phosphadecalin 3-oxides (= 3-(2,4-dinitrophenoxy)-2,4-dioxa-3-phosphabicyclo[4.4.0]decane 3-oxides = 2-(2,4-dinitrophenoxy)hexahydro-4*H*-1,3,2-benzodioxaphosphorin 2-oxides) have shown that the stereochemical course of the inhibition reaction is dependent on the substrate [1][2][1]). The general concept is summarized in *Scheme 1*, and the key spectroscopic features for the assignment of the configuration at the P-atom are outlined in *Scheme 2* (left)[2]). Accordingly, the existence of covalent O–P bonds between Ser^{195} of the enzyme and the inhibitors, *i.e.*, 'Ser^{195}' (CH_2O-P), has been anticipated due to the similarity of the chemical shifts of the phosphorylated enzyme sample with those of model compounds. This most probable but not fully unambiguous assumption has recently been verified by a preliminary experiment based on the concept depicted in *Scheme 2* [5][3]): The direct evidence of a covalent bond is the

---

[1]) For a full account on the background of the project, its context, and pertinent references, see [1][3].

[2]) The magnitude of the vicinal ^3J(P,H) is the key argument in assigning the conformation of the heterocyclic ring and, as a consequence, the configuration at the P-atom (*Scheme 2*) (see [1][2][4] and refs. cit. therein). In addition, the ^{31}P-NMR resonance of the axial P(3)-epimers is diamagnetically shifted with respect to their equatorially substituted counterparts.

[3]) Although the concept has been presented [5], it is recapitulated for the detailed, concluding report on that subject. Notice that for convenience, the implied CH_2O moiety of ^{195}Ser of the enzyme, *i.e.*, 'Ser^{195}'(CH_2O), is represented in *Figures* and *Schemes* by Ser^{195}O, Ser$^{195}-OCH_2$, or CT–Ser^{195}O (CT = δ-chymotrypsin).

Scheme 1

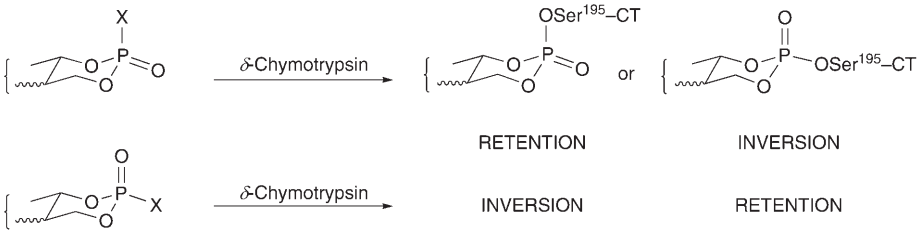

cis- and *trans*-decalins
X = electron withdrawing group, *e.g.*, F, Cl, 2,4-dinitrophenoxy
CT = Chymotrypsin

Scheme 2

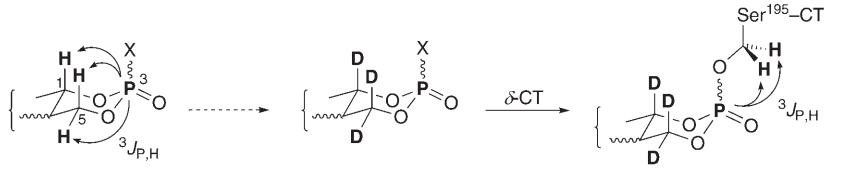

$\delta(^{31}P)_{ax} < \delta(^{31}P)_{eq}$

ax: *d*, $^3J(P,H_{eq}–C(5)) \approx 25$ Hz

eq: *t*, $^3J(P,H_{ax}–C(5)) \approx 11$ Hz

$^3J(P,H_{eq}–C(5)) \approx 11$ Hz

^{1}H-Coupled $^{31}P\{^2H\}$-NMR-spectra: Existence of a covalent bond between the inhibitor and serine^{195} of δ-chymotrypsin

existence of a vicinal coupling (^3J) between the P-atom of the inhibitor and the 'Ser^{195}'(CH_2O) of the enzyme. In principle, this coupling can be observed in the ^{1}H-coupled ^{31}P-NMR spectra, but the splitting caused *a priori* by H–C(1) and CH_2(5) of the oxaphosphadecalin interferes and makes an authentic monitoring difficult. Hence, the crucial ^3J(P,H) can be detected reliably only when all couplings with the ^{1}H-atoms of the inhibitor are supressed. This is accomplished by replacing them by ^{2}H-atoms. However, since ^{2}H also couples with the ^{31}P-atom[4]), $^{31}P\{^2H\}$-NMR spectra have to be recorded[5]) to obtain unequivocal information. This prerequisite is unfavorable with respect to the expected intensities of the resonances because coupling of ^{31}P with ^{1}H and quadrupol relaxation (^{2}H) significantly decrease the intensity of the signals.

---

[4]) This holds at least for the 1D spectra. Sophisticated 2D experiments would allow to avoid that particular problem, but as the δ values of H–C(1) and CH_2(5) in the ^{1}H-isomers of **9**–**12** are close to the 'Ser^{195}'(CH_2O), recording $^{31}P\{^2H\}$-spectra was considered to be the most straightforward approach. In general, coupling with nuclei of different quantum numbers causes complex splitting patterns which render the interpretation difficult. Although $^3J(P,^2H)$ is usually negligibly small and would only contribute to line broadening, it becomes significant in the present case ($^3J(P,H_{eq}–C(5)) \approx 25$ Hz and the expected $^3J(P,^2H_{eq}–C(5)) \approx 3.5$ Hz).

[5]) Since the ^{2}H-channel is usually the lock signal, this requirement is not trivial.

The preliminary experiment was performed with the axially *P*-substituted (±)-*trans*-3-(2,4-dinitrophenoxy)-2,4-dioxa-3-phospha(1,5,5-$^2H_3$)bicyclo[4.4.0]decane 3-oxide ((±)-**9a**) [5]. It demonstrated the feasibility of the concept and confirmed the stereochemical course in terms of inversion of the configuration at the P-atom as found [1]. However, due to the application of racemic inhibitors, two diastereoisomeric phosphorylated enzyme samples are generated *a priori*, a fact that further decreases the sensitivity of the experiment and complicates its interpretation. To increase the sensitivity and, in particular, to improve the significance of the method, we decided to investigate enantiomerically pure 1,5,5-trideuterated inhibitors. In addition to the 3-(2,4-dinitrophenoxy)(1,5,5-$^2H_3$) compounds **9** and **10** (*cf. Scheme 4*), also the corresponding cyclic (1,5,5-$^2H_3$)-3-fluoridates **11** and **12** (*cf. Scheme 4*) were prepared and investigated.

2. Synthesis and Characterization of the Deuterated Phosphadecalins. – 2.1. *Starting ($^2H_3$)Alcohols* **4** *and* **5**. The enantiomerically pure diols (+)- and (−)-**4**, and (+)- and (−)-**5**, resp.), were obtained after reduction of ethyl 2-oxocyclohexanecarboxylate (**1**) with $NaBD_4$ and chromatographic separation of the resulting ethyl (±)-*trans*- and (±)-*cis*-2-hydroxy(2-$^2H_1$)cyclohexanecarboxylates ((±)-**2** and (±)-**3**, resp.; *Scheme 3*). After reduction of the hydroxy esters (±)-**2** and (±)-**3** with $LiAlD_4$, the *trans*-diol (±)-**4** was esterified with (−)-(1*S*)-camphanoyl chloride to yield the mixture (*ca.* 1:1) of the diastereoisomeric bis-camphanates **6**/**7**[6]), and the *cis*-diol (±)-**5** was transformed into the bis-4-bromobenzoate (±)-**8** (= **8**/*ent*-**8**). Prep. HPLC (*Chiralcel® OD*) of **6**/**7** afforded **6** and **7** (de > 99%), and the same procedure with (±)-**8** gave **8** and *ent*-**8** (ee > 99%). Saponification of **6** and **7** afforded the *trans*-configurated (+)-(1*R*,2*S*)- and (−)-(1*S*,2*R*)-2-hydroxy(2-$^2H_1$)cyclohexane(α,α-$^2H_2$)methanols ((+)-**4** and (−)-**4**, resp.; ee > 99%). Saponification of **8** and *ent*-**8** gave the *cis*-configurated (+)-(1*S*,2*S*)- and (−)-(1*R*,2*R*)-2-hydroxy(2-$^2H_1$)cyclohexane(α,α-$^2H_2$)methanols ((+)-**5** and (−)-**5**, resp., ee > 99%).

The absolute configurations of the ($^2H_3$)diols were established independently with respect to the ^{1}H-isomers[7]) by X-ray crystallographic analyses. In the case of the *trans*-bis-camphanates **6** and **7**, the absolute configuration of the parent diols (+)- and (−)-**4**, respectively, was inferred *via* the (1*S*)-camphanoyl moiety, whereas the *cis*-bis-4-

---

[6]) It is remarkable that diastereoisomer **7** (1*S*,1′*S*,2′*R*) partly crystallized (de > 99%), whereas its enantiomer *ent*-**7** (1*R*,1′*R*,2′*S*), derivatized with (+)-(1*R*)-camphanoyl chloride, did not crystallize from the mixture (see *Exper. Part*). This unexpected fact made a simple separation of the enantiomers impossible.

[7]) The preparation and characterization of the optically active ^{1}H-isomeric *trans*- and *cis*-diols was reported earlier [1][2]. The procedures and the assignments of the absolute configurations had been performed according to [6] despite several inconsistencies, mainly concerning the magnitude of the optical rotations. The absolute configurations were unambiguously confirmed by X-ray crystallographic analyses of the corresponding phosphoramidates that had been obtained after derivatization of the optically active *cis*- and *trans*-configurated 3-chloro-2,4-dioxa-3-phosphabicyclo[4.4.0]decane 3-oxides with (+)-(*R*)- and (−)-(*S*)-(1-phenylethyl)amine [7].

Scheme 3

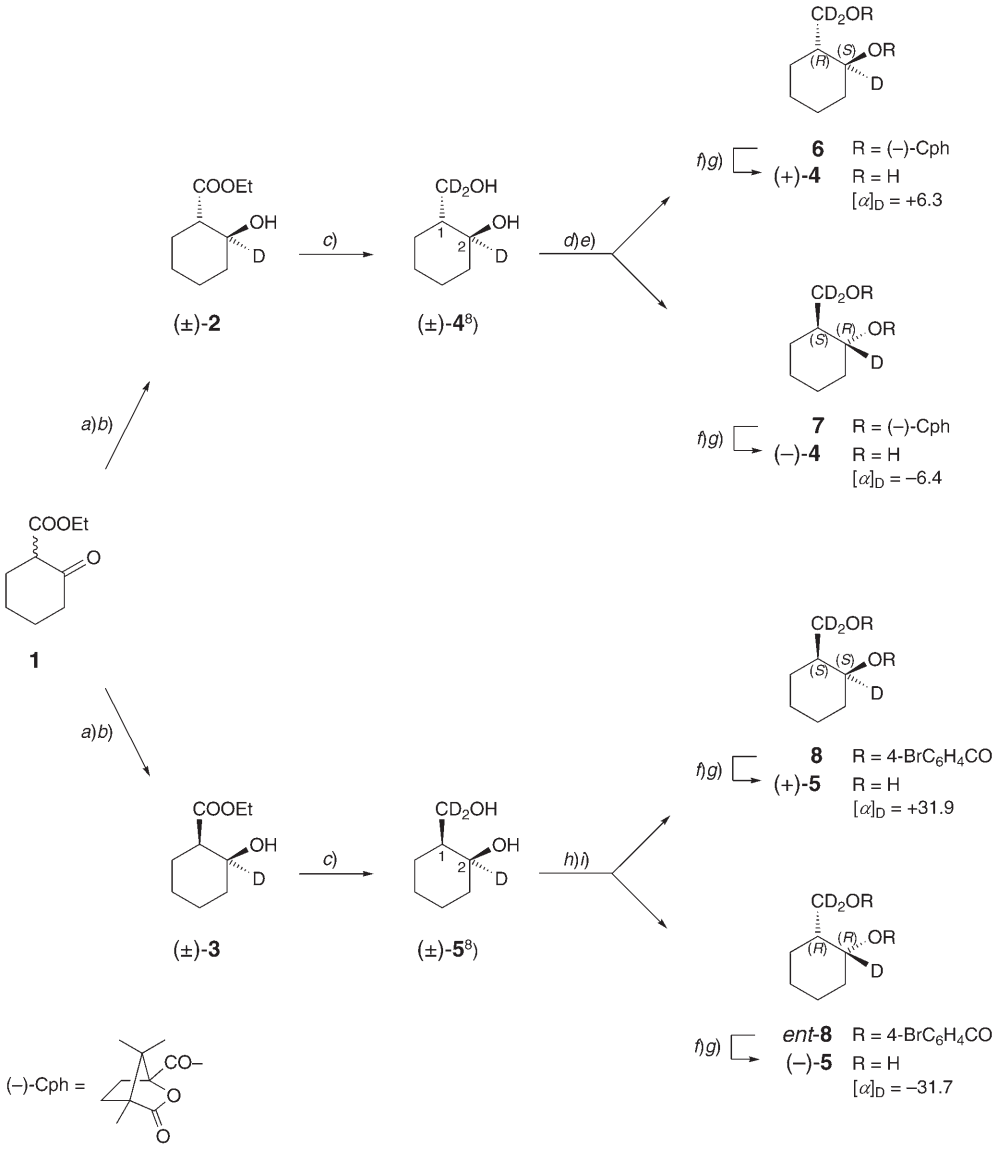

a) $NaBD_4$, EtOH, reflux (*cis*/*trans ca.* 3 :2 from **1**). *b*) CC (SiO_2, hexane/Et_2O). *c*) $LiAlD_4$, Et_2O, reflux. *d*) (−)-(1*S*)-Camphanoyl chloride, *N*,*N*-dimethylpyridin-4-amine (DMAP), pyridine, reflux. *e*) Prep. HPLC (*Chiralcel® OD*, hexane/MeOH/EtOH). *f*) $LiAlH_4$, THF, 0° → r.t. *g*) CC (SiO_2, CH_2Cl_2, AcOEt). *h*) 4-BrC_6H_6COCl, DMAP, pyridine, reflux. *i*) Prep. HPLC (*Chiralcel® OD*, hexane/EtOH).

---

[8]) According to *Chem. Abstr.*, the diols are substituted methanols. The IUPAC numbering system is different as it considers the same compounds as substituted cyclohexanols.

bromobenzoates **8** and *ent*-**8** enabled a direct determination due to the presence of the Br-atoms[9]). It is worth mentioning that the signs of the optical rotations and the absolute configurations of the ($^2H_3$)diols and the ^{1}H-isomers are coincident.

2.2. *3-Substituted 2,4-Dioxa-3-phosphadecalins* **9**–**12**, **14**, *and* **15**. The *trans*-2,4-dioxa-3-phospha(1,5,5-$^2H_3$)bicyclo[4.4.0]decane 3-oxides **9a**, **9b**, **11a**, and **11b** (*Scheme 4*) were prepared from (+)- or (−)-**4** by reaction with the appropriate phosphorus reagent (2,4-dinitrophenyl phosphorodichloridate for **9** and $POFCl_2$ for **11**) and chromatographic separation of the resulting P(3)-epimer mixture (axial/equatorial *ca.* 1:1) into the pure axial (**9a** and **11a**) and equatorial epimers (**9b** and **11b**). Similarly, starting from (+)- or (−)-**5**, the 3-substituted *cis*-2,4-dioxa-3-phospha(1,5,5-$^2H_3$)bicyclo[4.4.0]decane 3-oxides **10a**, **10b**, **12a**, and **12b** were obtained (*Scheme 4*). With respect to the ^{1}H-isomers [1][2][8], the sign of the optical rotations of all optically active 3-phospha(1,5,5-$^2H_3$)decalins remained unchanged, only the absolute values varied to some extent.

The *trans*- and *cis*-, axially and equatorially 3-substituted phosphoserine model compounds **14a**/**14a′** and **14b**/**14b′** (*trans*), and **15a**/**15a′** and **15b**/**15b′** (*cis*) were prepared from (±)-**4** and (±)-**5**, respectively, by reaction with *in situ* generated *N*-[(benzyloxy)carbonyl]-*O*-(dichlorophosphinyl)-L-serine methyl ester (**13**) and obtained as a mixture of diastereoisomers (*ca.* 1:1) after chromatographic separation (*Scheme 5*).

The NMR data of the 2,4-dioxa-3-phospha(1,5,5-$^2H_3$)decalins **9**–**12**, **14**, and **15** fully confirmed their structures (see *Exper. Part*). Significant ^{1}H- and ^{13}C-NMR characteristics are both the lack of the *ABX*-P-system in the heterocyclic moiety, and, due to ^1J(C,^{2}H) and ^2J(C,P), the complex *m* of C(1) and C(5) in **9**–**12** and of C(1′) and C(5′) in **14** and **15**, which hardly exceed the noise. Compared to the ^{1}H-isomers [1][2][8], δ(^{31}P) remained almost unchanged, the axially substituted epimers resonating at higher field with respect to the equatorially substituted counterparts. The decisive spectral feature is provided by the ^{31}P{^{2}H}-NMR spectra ($CDCl_3$) that exhibit a *t* at δ −6.66 (^3J(P,CH_2(3)) = 7.1 Hz)[10]) for **14a**/**14a′** and two *t* at δ −4.11 and −4.13 (^3J(P,CH_2(3)) = 6.5 Hz)[10]) for **14b**/**14b′**. The ^{1}H-correlated ^{31}P{^{2}H}-NMR spectra, as exemplified for the *trans*-isomers (*Fig. 1*), clearly showed the respective cross-peaks with H_A–C(3) and H_B–C(3) of the serine moiety at δ 4.50 and 4.39 (**14a**/**14a′**) and at δ 4.51 and 4.37 (**14b**/**14b′**), and also indicated a ^4J(P,H–C(2)) coupling at δ 4.57 in the case of **14b**/**14b′**. The same features hold for the *cis*-configurated model compounds **15a**/**15a′** (δ −6.49 (*m*, $w_{1/2} \approx 22$ Hz)) and **15b**/**15b′** (δ −3.93 (*m*, $w_{1/2} \approx 20$ Hz))[11]) (*Scheme 5*). In addition, significant ^4J(P,CH_2(10)) couplings are observed at δ 1.34–1.43 (**15a**/**15a′**) and at δ 1.52 (**15b**/**15b′**). To compare the chemical shifts with the conditions of the enzyme experiments, the spectra of the model compounds were also

---

[9]) The X-ray crystallographic analyses were performed by PD Dr. *A. Linden*, X-ray department of our institute. CCDC-650295–CCDC-650298 contain the full crystallographic data for the compounds **6**, **7**, **8**, and *ent*-**8**. These data can be obtained free of charge from the *Cambridge Crystallographic Data Centre*, *via* http://www.ccdc.cam.ac.uk/data_request/cif.

[10]) The signal is accidentally a *t* as H_A– and H_B–C(3) are diastereotopic.

[11]) Contrary to **14a**/**14a′** and **14b**/**14b′**, the *cis*-configurated model compounds **15a**/**15a′** and **15b**/**15b′** displayed only marginally resolved ^{31}P{^{2}H}-NMR spectra.

Scheme 4

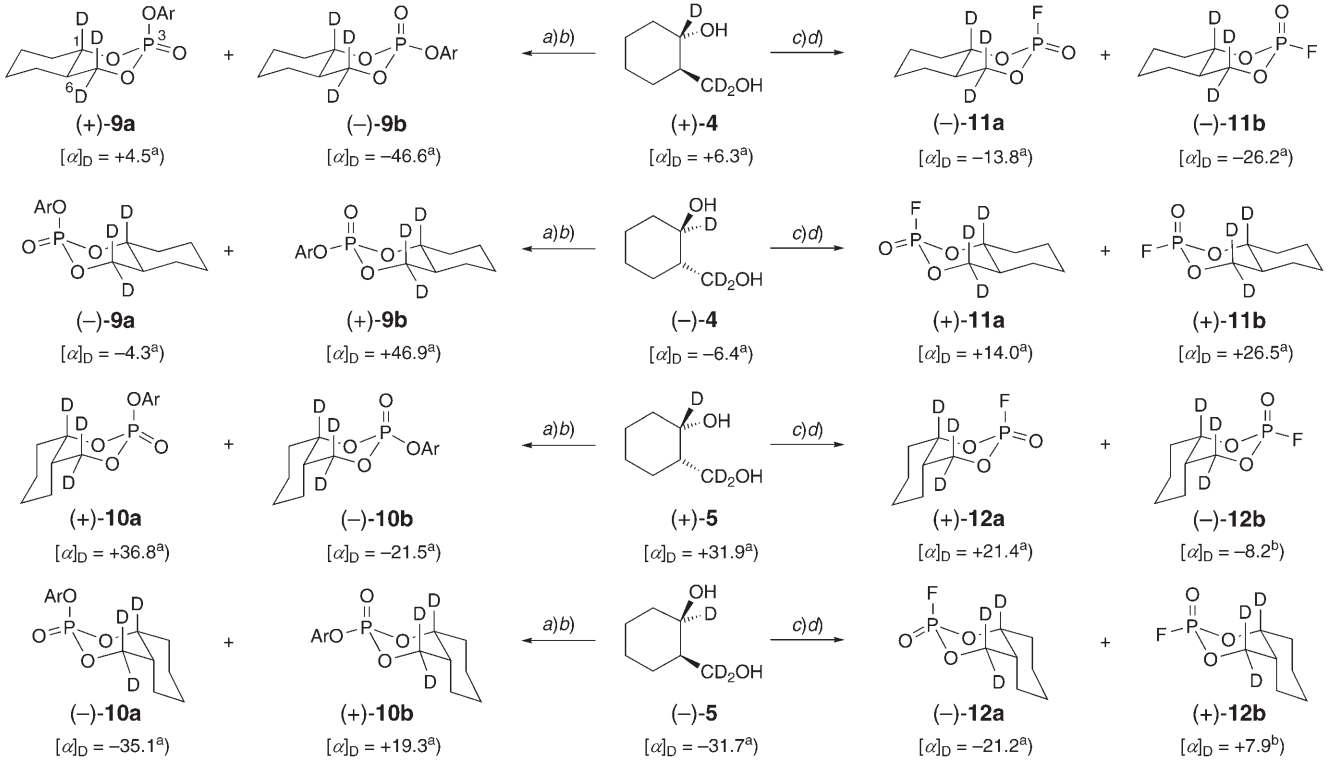

Ar = 2,4-$(NO_2)_2C_6H_3$

a) In $CHCl_3$ ($c = 1.00$). b) In acetone ($c = 1.00$); epimerization in $CHCl_3$.

a) $Cl_2P(O)C_6H_3(NO_2)_2$, pyridine, $CHCl_3$, 0° → r.t. *b*) CC (SiO_2, hexane/AcOEt). *c*) $Cl_2P(O)F$, pyridine, 0°. *d*) CC (SiO_2, hexane/Et_2O).

Scheme 5

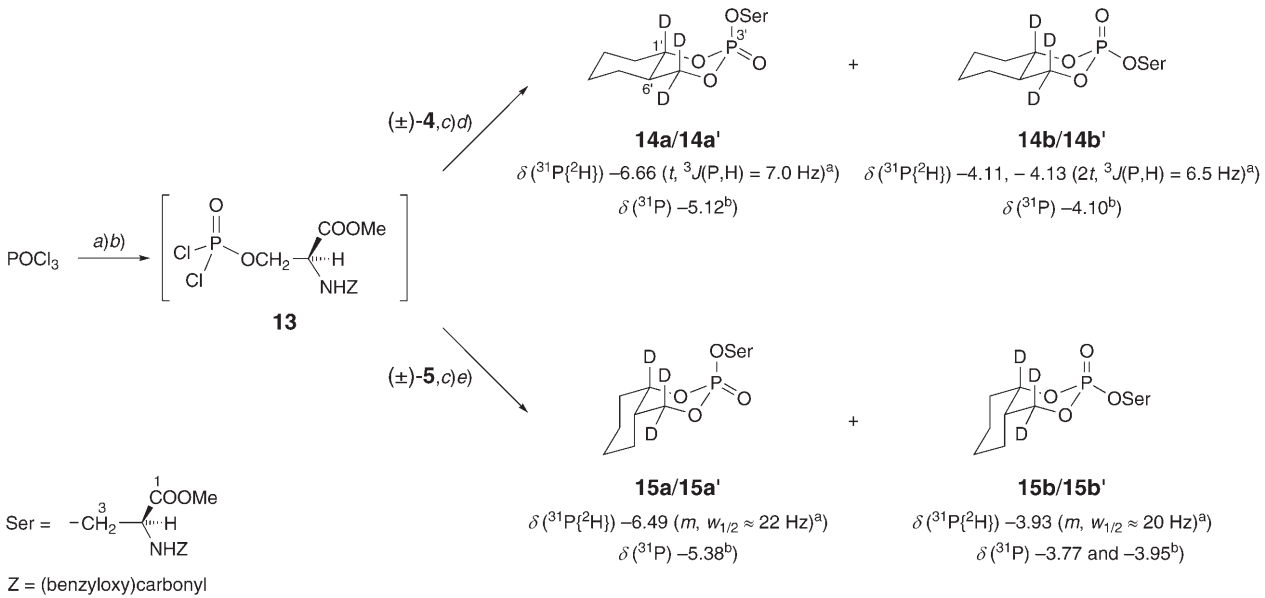

a) In $CDCl_3$. b) In CD_3CN/D_2O/0.2M *Tris* (pH 7.8).

a) Pyridine, Et_2O, 0°. *b*) (+)-*N*-[(Benzyloxy)carbonyl]-L-serine methyl ester, Et_2O, 0°, 2 h. *c*) Pyridine, Et_2O, r.t., 12 h. *d*) CC (SiO_2, $CHCl_3$/AcOEt).

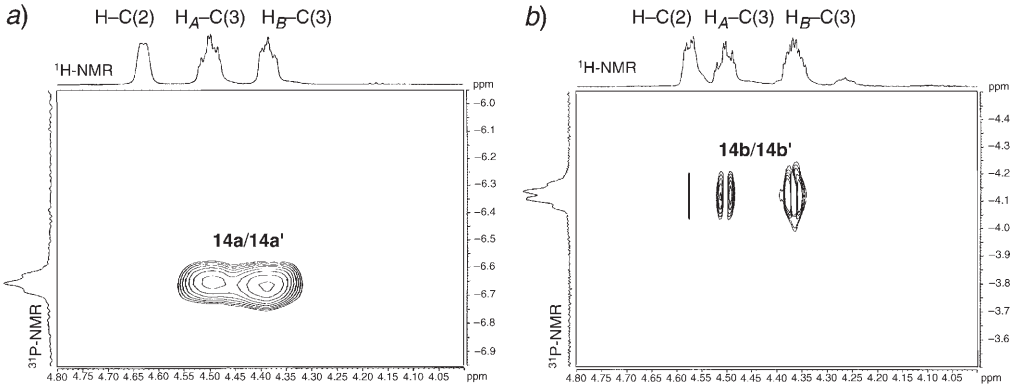

Fig. 1. *^{1}H-Correlated ^{31}P{^{2}H}-NMR spectra* ($CDCl_3$, 242.9 MHz, 27°) *of the model compounds* a) **14a**/**14a′** *and* b) **14b**/**14b′**

recorded in CD_3CN/D_2O/0.2M *Tris* (pH 7.8) 11:44:45. The respective $\delta(^{31}P)$ are −5.12 (**14a**/**14a′**), −4.10 (**14b**/**14b′**), −5.38 (**15a**/**15a′**), and −3.77 and −3.95 (**15b**/**15b′**) (*Scheme 5*).

3. Results of the ^{31}P-NMR Investigations. – 3.1. *General.* In analogy to the preceding setups [1][2], the experiments were designed so that δ-chymotrypsin and the inhibitors **9**–**12** reacted in stoichiometric amounts (*ca.* 2 μmol in *Tris* buffer at pH 7.8 and 27°). For the reason of the expected low sensitivity, the progression of the inhibition reaction was not spectroscopically tracked as in [1], and the NMR spectra were recorded only after complete inhibition had taken place. As observed in the preliminary experiment [5], the resolution of the 1D ^{31}P-NMR spectra was too low to reliably evidence the crucial ^3J(P,H) splitting. The existence of covalent bonds was decisively demonstrated by the 2D ^{1}H-correlated ^{31}P{^{2}H}-NMR spectra that reveal cross-peaks of the P-atoms of the inhibitors with the ^{1}H-resonances at δ *ca.* 4.1–4.5. According to the ^{1}H-NMR chemical shifts of the model compounds **14a**/**14a′**, **14b**/**14b′**, **15a**/**15a′**, and **15b**/**15b′**, this signal group is allocated to the 'Ser^{195}'(CH_2O). Despite the fact that the ^{31}P-NMR resonances did not very well agree with those of the model compounds, they were consistent within a series, and all the conclusions could be drawn unambiguously. In particular, the diamagnetic and the paramagnetic displacements could always be distinguished and clearly assigned to the corresponding axially or equatorially substituted phosphorylated enzyme species. This is well demonstrated in the 3-fluoro series where the inhibition did not proceed stereospecifically in most cases. But the respective Δδ values were always consistent.

3.2. *3-(2,4-Dinitrophenoxy) Inhibitors* **9** *and* **10**. The 2D ^{31}P,^{1}H-NMR spectra of the irreversible inhibition of δ-chymotrypsin with the enantiomerically pure *trans*- and *cis*-configurated, axially and equatorially 3-substituted 3-(2,4-dinitrophenoxy) derivatives **9** and **10** are compiled in the *Figs. 2–4*, and the interpretation of the stereochemical course is depicted in *Schemes 6–8*. After reaction of the enzyme with the *trans*-configurated compounds (+)- and (−)-**9a** and (+)- and (−)-**9b**, and with the *cis*-configurated (−)-**10b**, distinct NMR signals were detected, but no signals could be

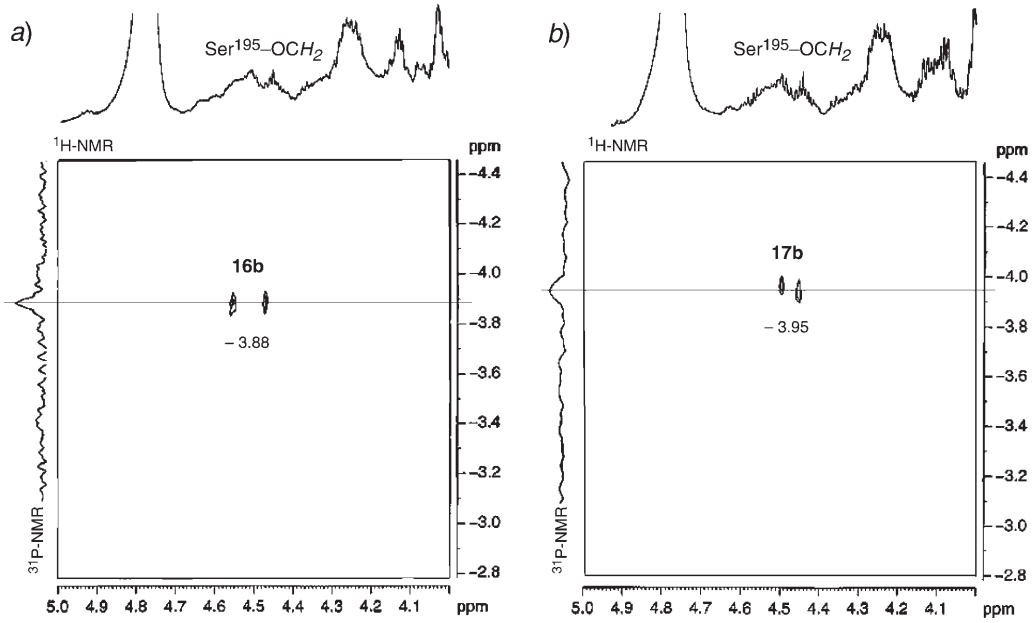

Fig. 2. *^1H-Correlated $^{31}P\{^2H\}$-NMR spectra* (242.9 MHz, 27°) *of the inhibition of δ-chymotrypsin with the* trans*-axial 3-(2,4-dinitrophenoxy)-3-phosphadecalins* a) *(+)*-**9a** *and* b) *(−)*-**9a**[3]). Solvent: 0.2M *Tris* buffer, pH 7.8, D_2O (44%), CD_3CN (11%).

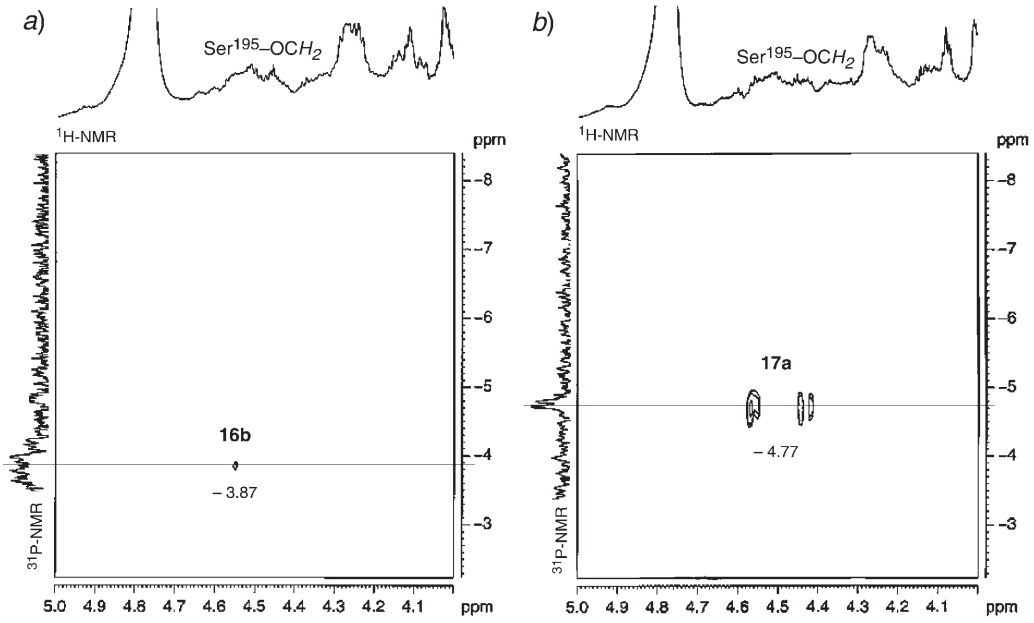

Fig. 3. *^1H-Correlated $^{31}P\{^2H\}$-NMR spectra* (242.9 MHz, 27°) *of the inhibition of δ-chymotrypsin with the* trans*-equatorial 3-(2,4-dinitrophenoxy)-3-phosphadecalins* a) *(−)*-**9b** *and* b) *(+)*-**9b**[3]). Solvent: 0.2M *Tris* buffer, pH 7.8, D_2O (44%), CD_3CN (11%).

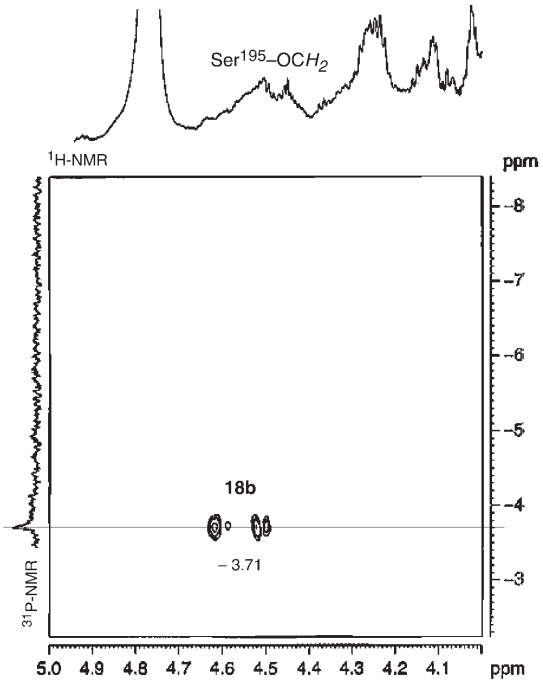

Fig. 4. *^{1}H-Correlated ^{31}P{^{2}H}-NMR spectrum* (242.9 MHz, 27°) *of the inhibition of δ-chymotrypsin with the* cis*-equatorial 3-(2,4-dinitrophenoxy)-3-phosphadecalin (–)-***10b**[3]). Solvent: 0.2M *Tris* buffer, pH 7.8, D_2O (44%), CD_3CN (11%).

Scheme 6

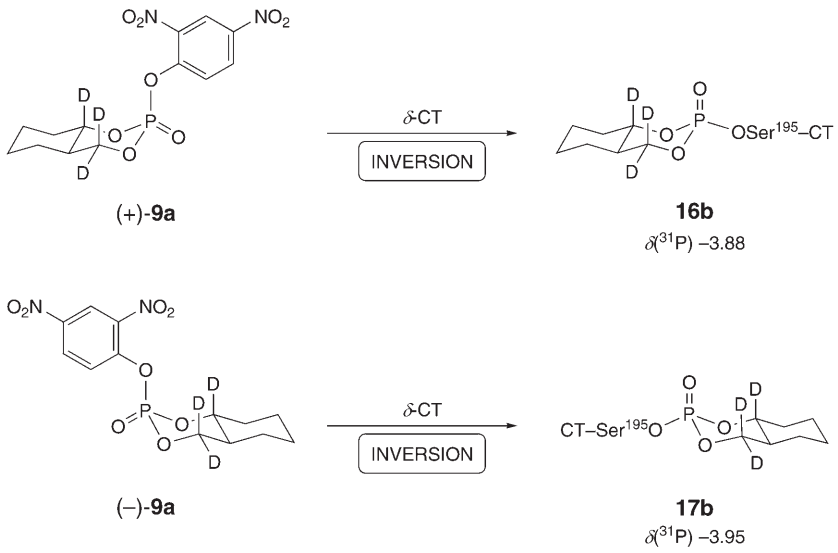

Scheme 7

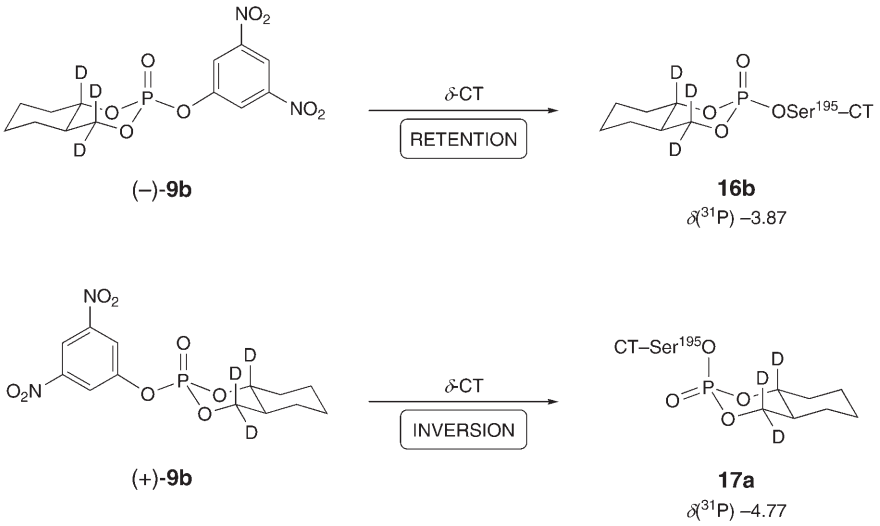

Scheme 8

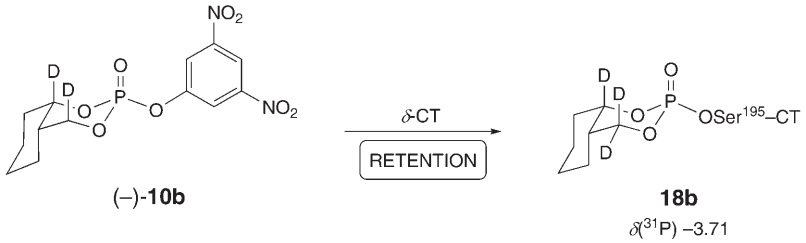

found when the enzyme was reacted with (+)- and (−)-**10a** and (+)-**10b**. This finding confirms the earlier results obtained with the ^{1}H-isomers [1][2]: It was shown kinetically and by ^{31}P-NMR spectroscopy that the four *trans*- and the (−)-*cis*-equatorial 3-(2,4-dinitrophenoxy)-3-phosphadecalins inhibited *δ*-chymotrypsin irreversibly, whereas the other *cis*-compounds turned out to be only weak reversible inhibitors.

Figs. 2–4 clearly demonstrate the reactions to proceed stereospecifically in terms of neat retention or inversion of the configuration at the P-atom. Reaction of the *trans*-configurated 3-axially substituted inhibitors (+)- and (−)-**9a** with *δ*-chymotrypsin gave ^{31}P,^{1}H-correlated signals at δ −3.88 and −3.95 (*Fig. 2*). Comparison of the ^{31}P-NMR chemical shifts with those of the *trans*-configurated model compounds **14a**/**14a′** (δ −5.12) and **14b**/**14b′** (δ −4.10) shows that these resonances can be attributed to the enzyme/inhibitor adducts in which the Ser^{195} moiety of *δ*-chymotrypsin occupies the equatorial position at the P-atom. Therefore, the diastereoisomeric structures **16b** and **17b** were assigned to the phosphorylated enzyme species, and, as a consequence, the inhibition reaction proceeded with inversion (*Scheme 6*). The same product **16b** (δ −3.87) was detected after inhibition of the enzyme with the *trans*-configurated 3-

equatorially substituted inhibitor (−)-**9b** (*Fig. 3,a*). On the other hand, reaction of its enantiomer (+)-**9b** yielded a high-field correlated signal at δ −4.77 (*Fig. 3,b*), characteristic for an axial substitution pattern at P(3). Therefore, structure **17a** was assigned to the inhibited enzyme. These findings are interpreted in terms of retention at P(3) with (−)-**9b** and inversion with (+)-**9b** to yield the reaction products **16b** and **17a** (*Scheme 7*). Inhibition of δ-chymotrypsin with the *cis*-configurated 3-equatorially substituted (−)-**10b** (the only irreversible inhibitor in the *cis*-series) gave rise to a low-field signal at δ −3.71 (*Fig. 4*), characteristic for equatorial substitution at P(3). In accordance with the *cis*-configurated model compounds **15a**/**15a′** (δ −5.38) and **15b**/**15b′** (δ −3.77 and −3.95), structure **18b** was deduced for the reaction product, and its formation can be explained by retention of the configuration at P(3) (*Scheme 8*).

Although the chemical shifts are slightly different from those reported, the results confirm the stereochemical course derived from the experiments with the ^{1}H-isomers [1][2][12]). In particular, the *trans*-axial compounds (+)- and (−)-**9a** react with inversion, the *trans*-equatorial congeners (+)- and (−)-**9b** with retention and inversion, and the *cis*-equatorial one ((−)-**10b**) with retention of the configuration at P(3).

3.3. *3-Fluoro Inhibitors* **11** *and* **12**. The results of the reaction of δ-chymotrypsin with the enantiomerically pure 3-phospha-3-fluoro derivatives **11** and **12** are depicted in the *Figs. 5–7* and in *Schemes 9–11*. After reaction of the enzyme with the *trans*-configurated compounds (+)- and (−)-**11a** and (+)- and (−)-**11b**, and with the *cis*-configurated (+)- and (−)-**12a**, the ^{31}P-NMR spectra showed these compounds to be

Scheme 9

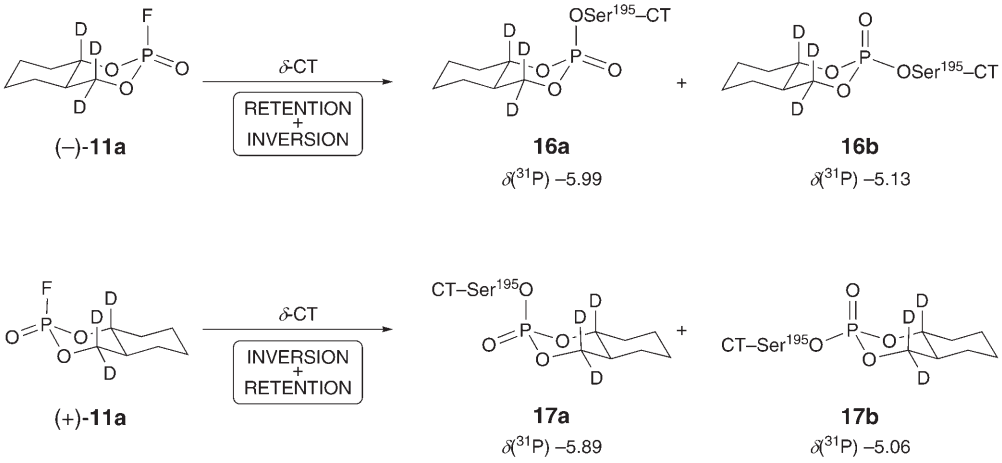

[12]) Generally, the δ(^{31}P) are shifted upfield by *ca.* 0.4–0.5 ppm with respect to those reported for the ^{1}H-isomers [1][2], but the respective relative differences between the P(3)-axially and P(3)-equatorially substituted species are consistent. In particular, the reliability of the interpretations is corroborated by the fact that the slower reacting enantiomer, *i.e.*, (−)-**9a**, of the *trans*-axial inhibitors gives rise to the paramagnetically shifted diastereoisomer, *i.e.*, **17b**, as described in [1].

Scheme 10

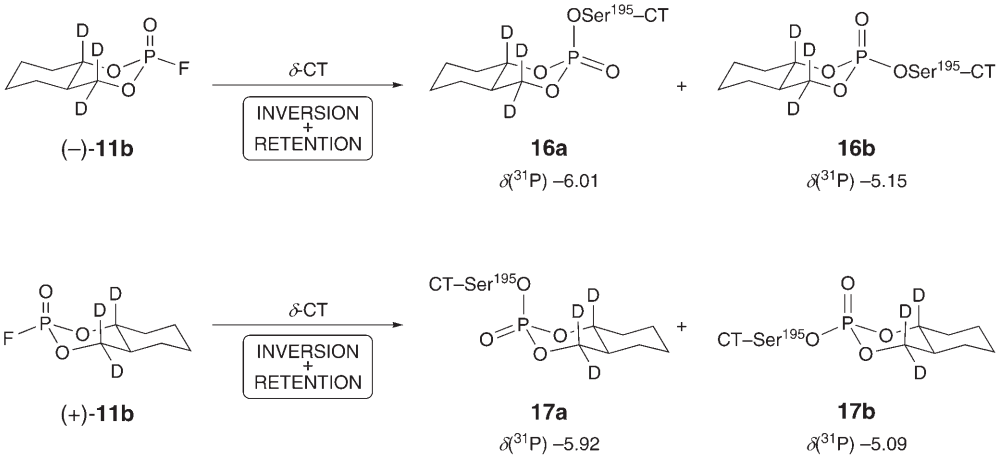

irreversible inhibitors (*Figs. 5–7*), whereas no signals could be detected when δ-chymotrypsin was treated with the *cis*-congeners (+)- and (−)-**12b**. *Figs. 5* and *6* reveal that the reactions with the four *trans*-configurated inhibitors give each rise to a pair of correlated peaks at δ −5.99 and −5.13, −5.89 and −5.06, −6.01 and −5.15, and −5.92 and −5.09, respectively. As discussed above, the diamagnetically shifted signals are indicative of axial substitution at P(3) (→diastereoisomeric phosphorylated enzyme species **16a** and **17a**) and the paramagnetically shifted ones for equatorial substitution at P(3) (→diastereoisomers **16b** and **17b**)[13]). This outcome clearly shows that the reactions do not proceed stereospecifically as both retention and inversion of the configuration at the P-atom take place (*Schemes 9* and *10*). On the other hand,

---

[13]) Formally, the phosphorylated diastereoisomeric enzymes **16a**, **16b**, **17a**, and **17b** originating either from the 2,4-dinitrophenoxy or the fluoro inhibitors (+)- and (−)-**9**, or (+)- and (−)-**11**, respectively (*Schemes 6* and *7*) are depicted as identical species. Hence, the respective pairs are expected to exhibit equal ^{31}P-chemical-shift displacements. However, although all the experiments were run under identical conditions, the compounds that are derived from the fluoro inhibitors **11** display upfield shifts ($\Delta\delta(^{31}P)$ *ca.* 1.2) with respect to those from the 2,4-dinitrophenoxy inhibitors **9**, a fact that needs a comment. Besides a non-controlled periodic change of the characteristics of the NMR probe-head, we definitely can rule out extrinsic factors that influence the chemical shift such as referencing, temperature, pH, and concentration. Since the ^{31}P-NMR resonances are consistent within an inhibitor series (**9** or **11**), we conclude that the P-atoms in the respective inhibited enzyme species are situated in a different environment. With regard to the characteristics of the leaving groups, we suppose that the properties of the F-atom are significantly different from those of the sterically and electronically demanding 2,4-dinitrophenoxy group, *i.e.*, the conformation of the active site and its environment are affected differently (actually in an unpredictable manner). Moreover, due to the structural features surrounding the catalytic triade such as the oxy-anion hole, further cationic and π-donor-type coordination sites [9], the 2,4-dinitrophenolate might remain embedded in the active-site pocket. However, this idea could not be corroborated by simple experiments with the model compounds, as $\delta(^{31}P)$ is invariable after adding various concentrations of 2,4-dinitrophenolate.

Scheme 11

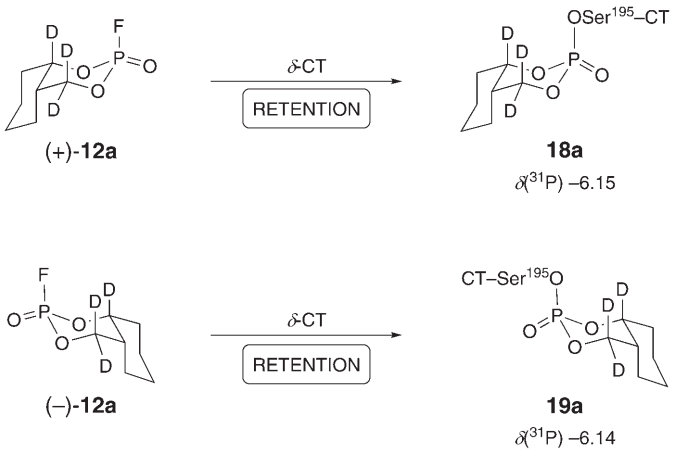

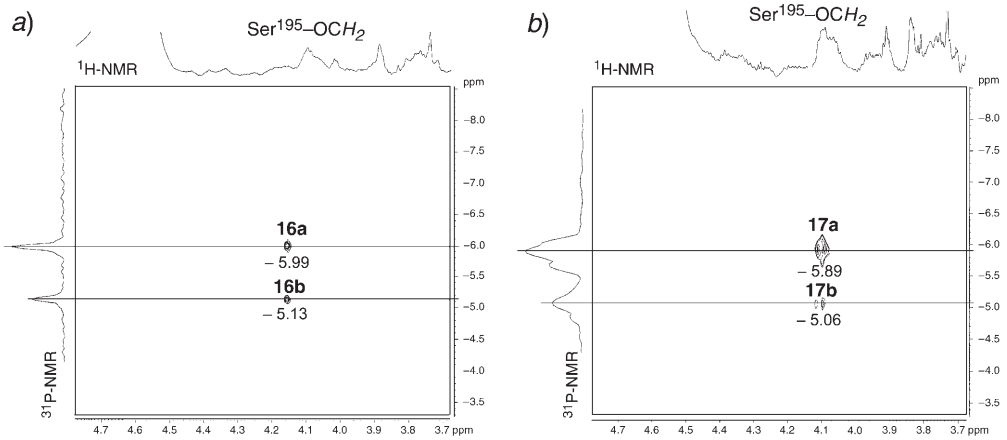

Fig. 5. *^{1}H-Correlated ^{31}P{^{2}H}-NMR spectra* (242.9 MHz, 27°) *of the inhibition of δ-chymotrypsin with the* trans*-axial 3-fluoro-3-phosphadecalins* a) *(–)*-**11a** *and* b) *(+)*-**11a**[3]). Solvent: 0.2M *Tris* buffer, pH 7.8, D_2O (44%), CD_3CN (11%).

inhibiton of δ-chymotrypsin with the *cis*-configurated 3-axially substituted congeners (+)- and (–)-**12a** gave rise to single correlated high-field signals at δ –6.15 and –6.14 (*Fig. 7*), characteristic for an axial substitution pattern at P(3). Hence, the reactions proceeded stereospecifically in terms of neat retention of the configuration at the P-atom to yield the diastereoisomeric phosphorylated enzyme species **18a** and **19a** (*Scheme 11*).

4. Interpretation of the Data and Conclusions. – 4.1. *General Mechanistic Considerations.* The mechanism of nucleophilic displacement reactions at a pentacoor-

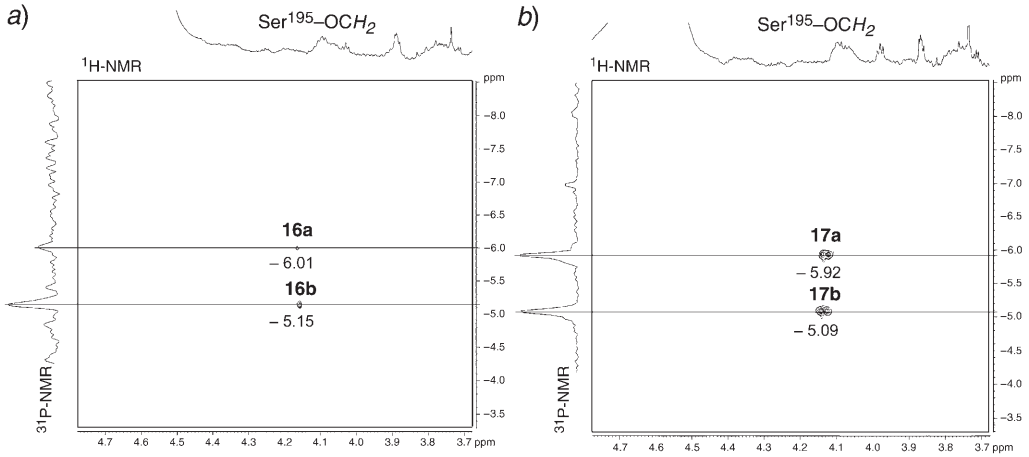

Fig. 6. *^{1}H-Correlated ^{31}P{^{2}H}-NMR spectra* (242.9 MHz, 27°) *of the inhibition of δ-chymotrypsin with the* trans*-equatorial 3-fluoro-3-phosphadecalins* a) *(−)*-**11b** *and* b) *(+)*-**11b**[3]). Solvent: 0.2M *Tris* buffer, pH 7.8, D_2O (44%), CD_3CN (11%).

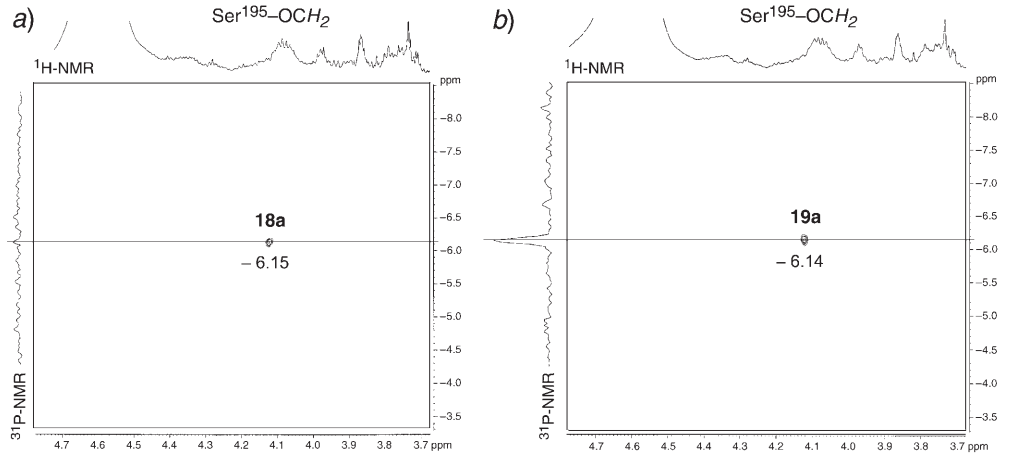

Fig. 7. *^{1}H-Correlated ^{31}P{^{2}H}-NMR spectra* (242.9 MHz, 27°) *of the inhibition of δ-chymotrypsin with the* cis*-axial 3-fluoro-3-phosphadecalins* a) *(+)*-**12a** *and* b) *(−)*-**12a**[3]). Solvent: 0.2M *Tris* buffer, pH 7.8, D_2O (44%), CD_3CN (11%).

dinate P-center such as phosphate esters and related compounds has been the subject of many fundamental studies from which conflicting results have emerged. In particular, exocyclic displacements occur with a bewildering variety of stereochemical implications, dependent on the nature of the substrate, attacking nucleophile, leaving group,

solvent, and further extrinsic factors[14]), and many results are equivocal. As a matter of fact, the stereochemistry of six-membered phosphorus-containing rings remains not completely understood [11][15]). Nonenzymic reactions of both five- and six-membered systems are comparable in wealth of mechanistic pathways available, including in-line and adjacent displacement mechanisms, pseudorotation of trigonal bipyramidal intermediates, and competing pathways. In comparable displacement reactions, retention at the P-atom is generally rationalized by an equatorial (adjacent) entry of the nucleophile followed by ligand reorganization (pseudorotation) according to their relative apicophilicities and apical departure of the leaving group [11][12]. In contrast, it was stated by *Westheimer* that all enzymic reactions at the P-atom proceed with inversion and, therefore, occur without pseudorotation [12]. In fact, there seems no unambiguous evidence that pseudorotation or adjacent attack at the P-atom is a significant process in any biological systems, and formal retention is rationalized by a multistep process with an even number of inversions [11–13].

4.2. *Rationalization of the Results.* Our investigations establish that the irreversible inhibition of δ-chymotrypsin is effected by covalent-bond formation between the nucleophilic O–C(β) of the active-site serine^{195} residue in the catalytic triade (Asp^{102} ⋯ His^{57} ⋯ Ser^{195}) in the enzyme [9] and the P-atom of the inhibitors. The phosphorylated enzyme is a stable tetrahedral adduct and considered to be an analogue of the tetrahedral carbonyl addition intermediate or its transition state [14].

The mechanistic rationalization in terms of S_N2(P)-type displacement processes is summarized in the *Schemes 12–14*. In-line apical attack (→ **A**) of the activated O–C(β) of Ser^{195} followed by apical departure of the leaving group from the pentacoordinated intermediate **B** [12] yields the equatorially substituted enzyme species (*e.g.*, **16b**) as found in the *trans*-axial series (*e.g.*, (+)-**9a** or (−)-**11a**); *Scheme 12*, left). In the *trans*-equatorial series (*e.g.*, (−)-**9b** or (−)-**11b**) an in-line attack of the nucleophile opposite to the leaving group is unfavored in the chair conformers, only an adjacent entry (→ **C**) [11][12] would be feasible (*Scheme 12*, middle). The arrangement of the substituents in the intermediate **D** where the leaving group is already in the required apical position enables its facile departure without prior pseudorotation (see *4.1*). The result of this process are the equatorially substituted phosphoenzymes (*e.g.*, **16b**) where the configuration at the P-atom is retained. According to stereoelectronic considerations (anomeric effect) which strongly favor the axial arrangement of an electronegative substituent, equatorially substituted cyclic phosphates preferentially adopt distorted conformations such as a boat (*e.g.*, (−)-**9b′** or (−)-**11b′**) or a twist-boat conformation (*e.g.*, (−)-**9b″** or (−)-**11b″**) [4]. Hence, the observed inversion can be explained by a direct in-line displacement process with these conformers (*via* intermediate **E**) during which the conformation in the trigonal bipyramid **F** may be maintained until the favorable chair is re-established from intermediate **G** yielding the

---

[14]) We have demonstrated that also the bulkiness of otherwise very similar auxiliary bases (DBN (=1,5-diazabicyclo[4.3.0]non-5-ene), DBU (=1,8-diazabicyclo[5.4.0]undec-7-ene) determines the stereochemical outcome of nucleophilic displacements at *trans*-3-chloro-2,4-dioxa-3-phosphabicyclo[4.4.0]decane 3-oxides [10].

[15]) The review [11] is the most comprehensive, critical paper covering several decades of research on this subject. Todate, no further significant contributions to this subject have appeared.

Scheme 12

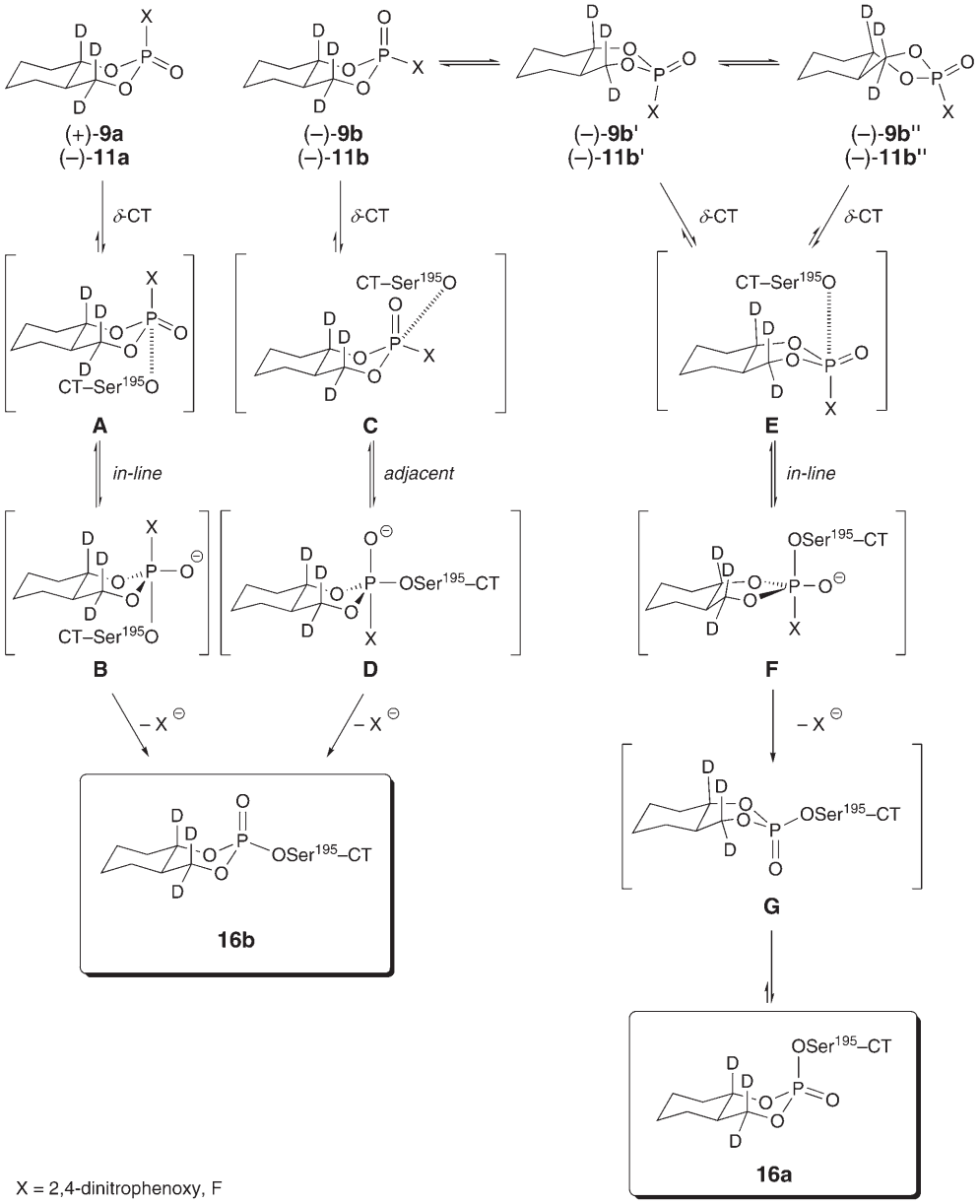

axially substituted phosphoenzymes (*e.g.*, **16a**, *Scheme 12*, right). We have no stringent explanation for the fact that (–)-**9b** reacts with retention (→**16b**, *Fig. 3*,*a*, and *Scheme 7*), whereas its enantiomer (+)-**9b** reacts with inversion of the configuration at

P(3) (→**17a**, *Fig. 3*,*b* and *Scheme 7*). However, since all these processes are strongly dependent on complex diastereoisomeric interactions, such results must never be excluded *a priori*[16]).

The situation in the conformationally flexible *cis*-series of the inhibitors is less straightforward (*Schemes 13* and *14*). The neat retention of (−)-**10b** can be explained by an adjacent displacement process (→**H**) *via* the intermediate **I** as discussed above (*Scheme 13*, left). The same argumentation considering the conformational changes associated with the anomeric effect would facilitate an in-line process with the conformers (−)-**10b′** and (−)-**10b″** and result in inversion of the configuration at the P-atom. However, besides these distorted conformations, also the completely ring-inverted double-chair conformer (−)-**10b‴** has to be regarded as a prominent substrate [4][8] (*Scheme 13*, right)[17]). It would enable a facile in-line attack (→**K**) to intermediate **L**, resulting in the equatorially phosphorylated enzyme species **18b‴**. From the experimental fact that no trace of a high-field ^{31}P-NMR signal corresponding to the axially substituted **18a** could be detected (see *Fig. 4*), we anticipate that **18b‴** might well be formed but does not undergo a complete ring inversion to **18a**, probably due to steric factors in the active-site pocket. As a consequence, this particular reaction sequence consists of two different inversion processes that result in overall retention.

Rationalizing the enzyme inhibition with the *cis*-fluoridates (+)- and (−)-**12a** (*Scheme 14*), it has to be expected *a priori* that an in-line attack (→**M**) would be feasible, leading to inversion of the configuation at P(3) *via* intermediate **N**. But the experimental results clearly show the reactions to proceed stereospecifically, and no trace of a low-field signal corresponding to an equatorial epimer (*e.g.*, **18b**) could be detected. Therefore, the reaction products have to be assigned to axially substituted phosphoenzymes (*e.g.*, **18a**). A possible explanation for the observed retention of the configuration at P(3) would be that an in-line attack (→**M**) from the 'bottom' side is hindered in the enzyme due to sterical crowding (*Scheme 14*, left), and only an adjacent attack (→**O**) *via* intermediate **P** and retention (→**18a**) takes place (*Scheme 14*, right).

5. Remarks. – As shown above, depending on the structure of the inhibitor, neat inversion, both inversion and retention, as well as neat retention of the configuration at the P-atom was found (*Schemes 6–11*). In particular, the stereochemical outcome of the inhibition depends not only on the configurational characteristics of the inhibitor as presented earlier [1][2] but also on the nature of the leaving group. This is exemplified

---

16) Such phenomena are not exceptional. It has been demonstrated earlier that the phosphonylation of α-lytic protease by P-epimeric hexapeptide analogues yields the same covalent adduct [15]. This result indicates inversion of the configuration at the P-atom for one diastereoisomer and retention for the other one. Although the authors are aware that displacement processes with pseudorotation are unprecedented in enzymic reactions, they consider it to be more plausible than a two-step mechanism.

17) Recently, the complete ring-inverted double-chair conformers of the (+)- and (−)-*cis*-3-fluoro-2,4-dioxa-3-phosphabicyclo[4.4.0]decane 3-oxides (the ^{1}H-isomers of (+)- and (−)-**12b**) have been evidenced by X-ray crystallographic analyses [8].

Scheme 13

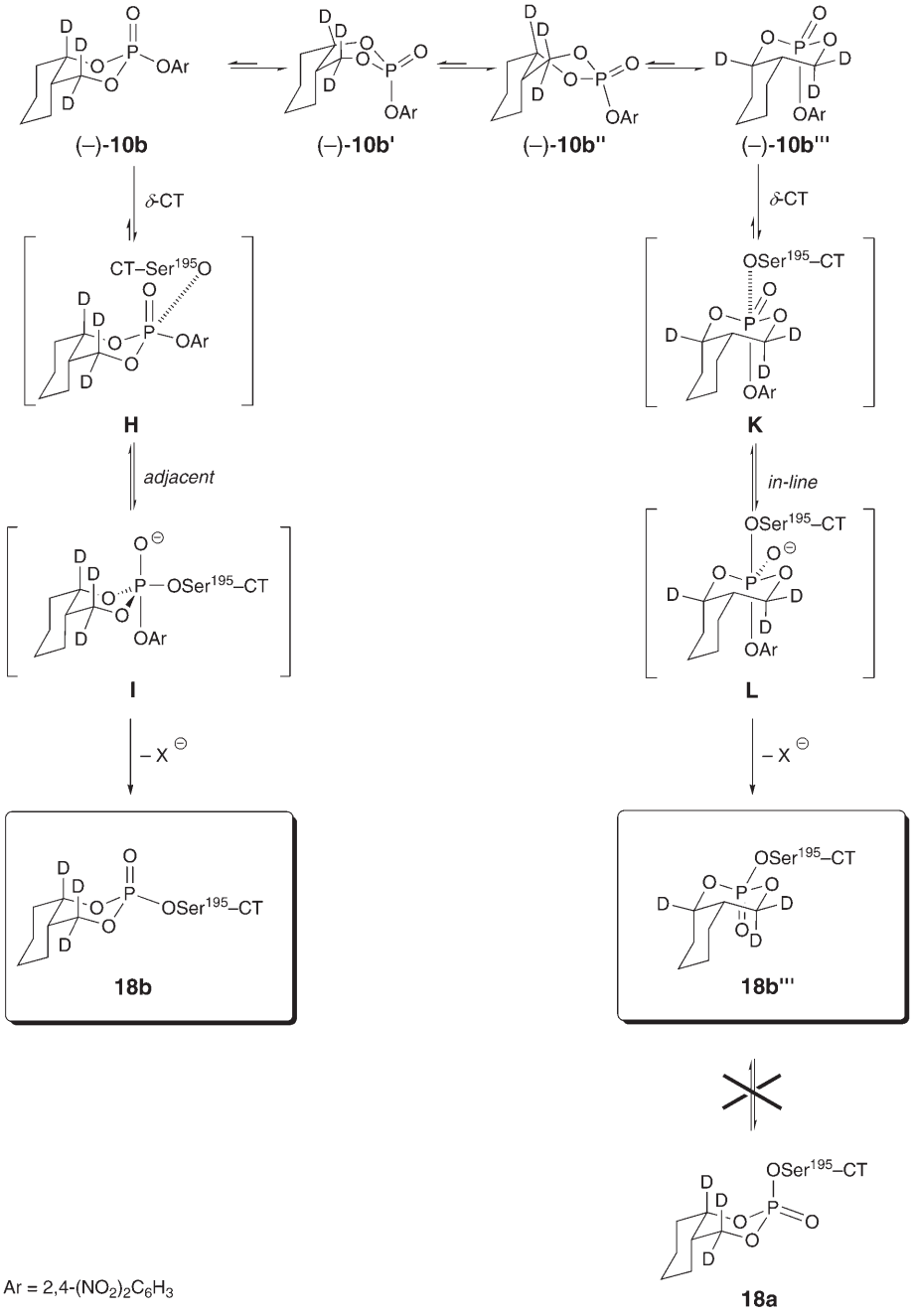
(–)-10b
(–)-10b'
(–)-10b''
(–)-10b'''
δ-CT
H
K
adjacent
in-line
I
L
– X⊖
18b
18b'''
18a
Ar = 2,4-(NO2)2C6H3

Scheme 14

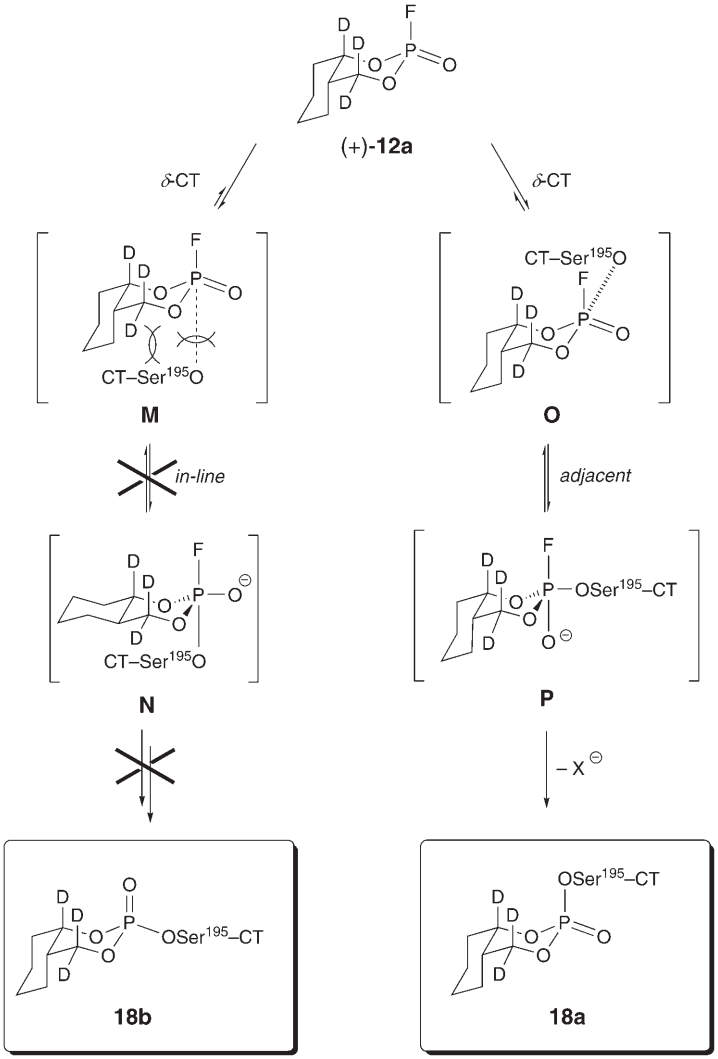

by the nonstereospecific reactions of the axially substituted *trans*-fluoridates (+)- and (−)-**11a**, in particular the partial retention of their configuration (*Scheme 9*). The latter fact cannot be explained by the actual argumentation. We are well aware that the real reaction pathways may be significantly more complex than the experiments make apparent. Hence, our approach is simplified as it does not consider postinhibitory phenomena [16] (*e.g.*, aging [17]) nor dynamic and kinetic processes. Thus, the inhibition might also be crucially determined by the dynamics of the active site and pre-

or postinhibitory epimerization of the phosphoenzymes to the most compatible stereoisomer[18]).

As a consequence, our interpretations remain with reservations and are based simply on the experimental data to the best of our knowledge. The presented results seem contradictory to the generally accepted knowledge that enzymatic mechanisms proceed stereospecifically. This holds indeed for biological processes that had been optimized by an evolutionary development but not necessarily for nonspecific substrates such as the investigated inhibitors.

We thank dipl. chem. *M. Wächter* for additional, clarifying experiments, PD Dr. *O. Zerbe*, Mrs. *N. Bross-Walch*, and *S. Jurt* from the NMR department of our institute for their continuous advice and help, and PD Dr. *A. Linden* for the X-ray crystallographic analyses. The financial support of the project by the *Swiss National Science Foundation* is gratefully acknowledged.

Experimental Part

1. *General*. See [1–3]. For the particular precautions in preparing and handling the organophosphates, see [3]. In addition: The camphanoyl derivatives were prepared with (+)-(1*R*)- and (−)-(1*S*)-camphanoyl chloride (=(+)-(1*R*,4*R*)- and (−)-(1*S*,4*R*)-4,7,7-trimethyl-3-oxo-2-oxabicyclo[2.2.1]-heptane-1-carbonyl chloride = *ChiraSelect Fluka 21286* and *21287*). $[\alpha]_D^{25}$: *Perkin-Elmer 241-MC* polarimeter with thermostat *B. Braun Thermomix 1441*; 10 cm cell; ee based on the integration of the peak areas of the anal. HPLC separations ($R_s > 1.5$). Anal. HPLC: *Chiralcel® OD-H* (*Daicel Chemical Industries, Ltd.*; 5 μ, 250 × 4.6 mm) column; flow rate 1 ml/min; at r.t.; *Pharmacia LKB* HPLC pump *2248*; *Hewlett-Packard 1040M* diode-array detection system; data handling with a *Hewlett-Packard* Chemstation for LC, Rev. A.04.02. Prep. HPLC: *Chiralcel® OD* (10 μ, 250 × 20 mm) column; flow rate 12 ml/min; at r.t.; *Applied-Biosystems 400* solvent delivery system; *Applied-Biosystems 783A* programmable absorbance detector.

2. *Ethyl (±)*-trans- *and (±)*-cis-*2-Hydroxy(2-$^2H_1$)cyclohexanecarboxylates* ((±)-**2** and (±)-**3**, resp.). To a cooled soln. (*ca.* 0°) of ethyl 2-oxocyclohexanecarboxylate (**1**) (16.6 g, 97.6 mmol) in anh. EtOH (250 ml), $NaBD_4$ (1.40 g, 33.4 mmol) was added in portions, and the mixture was kept for 3 h at *ca.* 0°. Workup and continuous extraction with Et_2O yielded (±)-**2**/(±)-**3** as a slightly greenish oil (15.62 g, 94%). CC (SiO_2, hexane/Et_2O 5:4) afforded pure (±)-**2** (*trans*-isomer; 5.29 g, 34%) and (±)-**3** (*cis*-isomer; 8.23 g, 53%) as colorless oils. Data: identical with those of (±)-**2** and (±)-**3** reported in [5].

3. *(±)*-trans *and (±)*-cis-*2-Hydroxy(2-$^2H_1$)cyclohexane(α,α-$^2H_2$)methanols* (=*(±)*-trans- *and (±)*-cis-*2-Hydroxy(2,2-$^2H_2$)methyl(1-$^2H_1$)cyclohexan-1-ols*; (±)-**4** and (±)-**5**, resp.). To a cooled soln. (*ca.* 0°) of (±)-**2** (5.29 g, 30.5 mmol) in anh. Et_2O (10 ml), $LiAlD_4$ (1.28 g, 30.5 mmol) was added in portions. After 40 min at 0°, the mixture was refluxed overnight, then usual workup and continuous extraction with Et_2O afforded the *trans*-diol (±)-**4** (2.76 g, 68%) as a white amorphous solid.

Starting from (±)-**3** (8.23g, 47.5 mmol) in Et_2O (150 ml) and $LiAlD_4$ (2.0 g, 47.5 mmol), the analogous procedure yielded the *cis*-diol (±)-**5** (5.42 g, 86%) as a colorless viscous oil that solidified in the refrigerator after distillation at 100°/1 Torr. Data: identical with those of (±)-**4** and (±)-**5** reported in [5].

4. *(+)-(1*R,2S*)- and (−)-(1*S,2R*)-2-Hydroxy(2-$^2H_1$)cyclohexane(α,α-$^2H_2$)methanols* ((+)- and (−)-**4**, resp.). 4.1. *Diastereoisomeric Bis-camphanoyl Derivatives* **6** *and* **7**. To a soln. of (±)-**4** (2.00 g, 15.04 mmol) in pyridine (100 ml) and DMAP (50 mg) at 60°, (−)-(1*S*)-camphanoyl chloride (6.53 g, 30.1 mmol) was added and the mixture refluxed for 18 h. After workup, treating the residue with charcoal/EtOH, and crystallization, the *ca.* 1:1 mixture of the diastereoisomers **6** (1*S*,1′*R*,2′*S*) and **7** (1*S*,1′*S*,2′*R*) was obtained as colorless crystals (6.89 g, 93%). Recrystallization from toluene afforded pure **7** (2.06 g, 30%; de > 99%)[6]). Repeated prep. HPLC of the mother liquor (*Chiralcel® OD*, hexane/MeOH/EtOH 20:1:0.1;

---

[18]) Several observations pointing towards that direction have been mentioned in [1][2]. Although planned, we did not investigate these phenomena thoroughly, mainly because they were partly accidental and transient and not really reproducible.

λ_{det} 220 nm; $\alpha = 1.21$; $R_s = 1.6$) afforded from the less polar fractions ($k' = 2.8$) pure **6** (3.32 g, 48%; de > 99%) and from the more polar ones ($k' = 3.4$) additional **7** (1.25 g, 18%; de > 99%).

When (±)-**4** was treated analogously with (+)-(1*R*)-camphanoyl chloride, *ent*-**7** (1*R*,1′*R*,2′*S*) did not crystallize as expected and prevented a simple enantiomer separation.

Data of (1S,4R)-4,7,7-Trimethyl-3-oxo-2-oxabicyclo[2.2.1]heptane-1-carboxylic Acid {(1R,2S)-2-{{[(1S,4R)-4,7,7-trimethyl-3-oxo-2-oxabicyclo[2.2.1]hept-1-yl]carbonyl}oxy}(2-$^1H_2$)cyclohexyl}($^2H_2$)-methyl Ester (**6**): Colorless needles. M.p. 165°. R_f (hexane/AcOEt 1:2) 0.45. UV/VIS (EtOH): 230. IR (KBr): 3557*w*, 3431*w*, 2971*s*, 2940*s*, 2870*s*, 1789*s*, 1725*s*, 1454*s*, 1276*s*, 1167*s*, 1103*s*, 1060*s*, 821*s*, 743*s*, 621*m*, 585*m*, 507*m*. ^{1}H-NMR (300 MHz, $CDCl_3$): 2.41 (*ddd*, $^2J = 13.4$, $^3J = 10.8$, 4.2, 2 H_{exo}–C(6)); 2.11–2.01 (*m*, 2 H_{endo}–C(6), H_{eq}–C(3′)); 1.96–1.86 (*m*, 2 CH_2(5)); 1.80–1.63 (*m*, H–C(1′), H_{eq}–C(6′), CH_2(4′)); 1.41–1.24 (*m*, H_{ax}–C(6′), CH_2(5′), H_{ax}–C(3′)); 1.11 (*s*, 1 Me–C(4)); 1.06, 1.05, 0.96 (each *s*, 1 Me–C(4), 4 Me–C(7)). ^{13}C-NMR (75.4 MHz, $CDCl_3$): 177.9 (C(3)); 167.3, 166.7 (*C*O–C(1)); 91.0 (C(1)); *ca*. 79 (*m*, C(2′))[19]); *ca*. 70 (*m*, *C*D_2OCamph.)[19]); 54.7 (C(4)); 54.0 (C(7)); 41.1 (C(1′)); 31.4 (C(3′)); 30.6 (C(6)); 28.8 (C(5)); 28.0 (C(6′)); 24.5 (C(5′)); 24.1 (C(4′)); 16.7, 16.6, 9.6 (*Me*–C(4), Me–C(7)). CI-MS (NH_3): 510 (100, $[M + NH_4]^+$, $[C_{27}H_{35}D_3O_8 + NH_4]^+$), 494 (15, $[M + H]^+$), 330 (12, $[M + NH_4 -$ Camph.$]^+$). ESI-MS (CH_2Cl_2/MeCN/NaI): 516 (100, $[M + Na]^+$, $[C_{27}H_{35}D_3O_8 + Na]^+$).

Data of (1S,4R)-4,7,7-Trimethyl-3-oxo-2-oxabicyclo[2.2.1]heptane-1-carboxylic Acid {(1S,2R)-2-{{[(1S,4R)-4,7,7-trimethyl-3-oxo-2-oxabicyclo[2.2.1]hept-1-yl]carbonyl}oxy}(2-$^2H_1$)cyclohexyl}($^2H_2$)-methyl Ester (**7**): Colorless cubes. M.p. 174°. R_f (hexane/AcOEt 1:2) 0.45. UV/VIS (EtOH): 230. IR (KBr): 3556*w*, 3435*w*, 2974*s*, 2943*s*, 2871*s*, 1785*s*, 1725*s*, 1454*s*, 1276*s*, 1167*s*, 1103*s*, 1060*s*, 821*s*, 743*s*, 621*m*, 585*m*, 507*m*. ^{1}H-NMR (300 MHz, $CDCl_3$): 2.43 (*ddd*, $^2J = 13.4$, $^3J = 10.8$, 4.2, 2 H_{exo}–C(6)); 2.12–1.80 (*m*, 2 H_{endo}–C(6), H_{eq}–C(3′), 2 CH_2(5)); 1.75–1.64 (*m*, H–C(1′), H_{eq}–C(6′), CH_2(4′)); 1.40–1.27 (*m*, H_{ax}–C(6′), CH_2(5′), H_{ax}–C(3′)); 1.11, 1.06, 0.97 (each *s*, 2 Me–C(4), 4 Me–C(7)). ^{13}C-NMR (75.4 MHz, $CDCl_3$)[20]): 177.9 (C(3)); 167.3, 166.7 (*C*O–C(1)); 91.0 (C(1)); 54.7 (C(4)); 54.0 (C(7)); 41.1 (C(1′)); 31.4 (C(3′)); 30.6 (C(6)); 28.9 (C(5)); 28.0 (C(6′)); 24.5 (C(5′)); 24.1 (C(4′)); 16.7, 16.6, 9.6 (*Me*–C(4), *Me*–C(7)). CI-MS (NH_3): 510 (100, $[M + NH_4]^+$, $[C_{27}H_{35}D_3O_8 + NH_4]^+$), 494 (18, $[M + H]^+$), 330 (15, $[M + NH_4 -$ Camph.$]^+$). ESI-MS (CH_2Cl_2/MeCN/NaI): 516 (100, $[M + Na]^+$, $[C_{27}H_{35}D_3O_8 + Na]^+$).

4.2. trans-*Diols* (+)- *and* (−)-**4**. To a cooled soln. (*ca.* 0°) of **6** (1.04 g, 2.11 mmol) in anh. THF (30 ml), $LiAlH_4$ (240 mg, 6.33 mmol) was slowly added in portions. After 30 min at 0°, the mixture was refluxed until no starting material was detected (TLC). Extraction with Et_2O and workup afforded a mixture of (+)-**5** (R_f (CH_2Cl_2/AcOEt 3:4) 0.12) and the reduction products of camphanic acid (R_f (CH_2Cl_2/AcOEt 3:4) 0.09) as a colorless viscous residue (916 mg). CC (SiO_2, CH_2Cl_2/AcOEt 3:4) afforded pure (+)-**4** (145 mg, 52%)[21]) as a colorless viscous oil that solidified in the refrigerator.

The analogous procedure, starting from **7** (1.16 g, 2.35 mmol) in THF (30 ml) and $LiAlH_4$ (270 mg, 7.1 mmol) yielded (−)-**4** (172 mg, 55%)[21]).

Data of (+)-**4**: White amorphous solid. M.p. 10–15°. R_f (AcOEt) 0.22. $[\alpha]_D^{25} = +6.3$ ($c = 1.00$, $CHCl_3$). IR (film): 3323*s* (br.), 2925*s*, 2853*s*, 2665*m*, 2197*m*, 2085*m*, 1650*w*, 1449*s*, 1412*s*, 1332*s*, 1147*s*, 1083*s*, 1002*s*, 961*s*, 906*m*, 855*m*, 817*m*, 484*s*. ^{1}H-NMR (300 MHz, $CDCl_3$): 3.83 (br. *s*, $w_{1/2} \approx 12$, 2 OH); 1.93 (*dd*, ^3J(1,6ax) = 12, ^3J(1,6eq) = 3, H–C(1)); 1.76–1.45 (*m*, H_{eq}–C(3), CH_2(4), H_{eq}–C(6)); 1.40–1.12 (*m*, CH_2(5), H_{ax}–C(3)); 0.91 (*qd*, $^2J \approx {}^3J$(6ax,1) $\approx {}^3J$(6ax,5ax) = 12, ^3J(6ax,5eq) = 3.6, H_{ax}–C(6)). ^{13}C-NMR: 75.6 (*t*-like, ^1J(C,^{2}H) = 21.3, C(2)); 67.5 (*quint.*-like, ^1J(C,^{2}H) = 21.5, CD_2OH); 45.8 (C(1)); 35.2 (C(3)); 27.3 (C(6)); 25.1 (C(5)); 24.5 (C(4)). EI-MS: 133 (1, M^+, $[C_7H_{11}D_3O_2]^+$), 115 (22, $[M - H_2O]^+$), 97 (55, $[M - 2\,H_2O]^+$), 81 (26), 70 (100), 58 (62).

Data of (−)-**4**: $[\alpha]_D^{25} = -6.4$ ($c = 1.00$, $CHCl_3$). All other data: identical with those of (+)-**4**.

---

[19]) Due to ^1J(C,^{2}H) and ^2J(C,P), the ^{2}H-substituted C-atoms gave rise to complex, not resolved *m* that hardly exceeded the noise.

[20]) The signals of the ^{2}H-substituted C-atoms did not exceed the noise and could not be detected.

[21]) Because the separation of the diols from the optically active reduction products of camphanic acid required laborious chromatography, only the very best fractions were pooled (GC control) to obtain an ee > 99%.

5. *(+)-(1S,2S)- and (−)-(1R,2R)-2-Hydroxy(2-$^2H_1$)cyclohexane(α,α-$^2H_2$)methanols* ((+)-**5** and (−)-**5**, resp.). 5.1. *Bis-4-bromobenzoate* (±)-**8** *and Enantiomers* **8** (1*S*,2*S*) *and* ent-**8** (1*R*,2*R*). To a soln. of (±)-**5** (2.45 g, 18.42 mmol) and DMAP (200 mg) in pyridine (100 ml), 4-bromobenzoyl chloride (8.55 g, 39 mmol) was added and the mixture refluxed overnight. After workup, the crude residue was subjected to CC (SiO_2, hexane/CH_2Cl_2/Et_2O 6:4:1): (±)-**8** (6.16 g, 67%) as colorless crystals. Repeated prep. HPLC (*Chiralcel® OD*, hexane/EtOH 12:1; λ_{det} 240 nm; $\alpha = 2.33$; $R_s > 6$) afforded from the less polar fractions ($k' = 1.2$) pure **8** (2.88 g; ee > 99%) and from the more polar ones ($k' = 2.8$) pure *ent*-**8** (2.91 g; ee > 99%).

Data of 4-Bromobenzoic Acid {[1S,2S)-2-[(4-Bromobenzoyl)oxy](2-$^2H_1$)cyclohexyl}($^2H_2$)methyl Ester (**8**): Colorless needles. M.p. 130.5°. R_f (hexane/CH_2Cl_2/Et_2O 4:6:1) 0.60. IR (KBr): 3407*w*, 2936*s*, 2799*m*, 1917*w*, 1791*m*, 1714v*s*, 1585*s*, 1267*s*, 1065*s*, 753*s*, 680*s*, 471*m*. ^{1}H-NMR (300 MHz, $CDCl_3$): 7.86 (*dd*, $^3J = 8.6$, $^4J = 1.9$, 2 H_o); 7.56 (*dd*, $^3J = 8.7$, $^4J = 1.9$, 2 H_m); 2.16 (*dd*, $^3J(1,6ax) = 10.3$, $^3J(1,6eq) = 4.2$, H−C(1)); 2.11–2.04 (*m*, H_{eq}−C(3)); 1.85 (*m*, *d*-like, $w_{1/2} \approx 20$, H_{ax}−C(3)); 1.78–1.39 (*m*, CH_2(4), CH_2(5), CH_2(6)). ^{13}C-NMR (75.4 MHz, $CDCl_3$)[20]: 165.6, 164.9 (CO); 131.7, 131.6 (C_o); 130.9 (C_m); 128.9 (C_p); 127.9 (C_{ipso}); 39.4 (C(1)); 29.6 (C(3)); 24.5 (C(6)); 24.2 (C(5)); 20.7 (C(4)). EI-MS: 501, 499, 497 (<1, 1, <1, $M(^{81}Br)^+$, $M(^{81}Br^{79}Br)^+$, $M(^{79}Br)^+$, $C_{21}H_{17}Br_2D_3O_4^+$); 299, 298, 297, 296 (6, 3, 6, 2, [M − $BrC_6H_4COO]^+$), 281 (5), 207 (10), 185 (78, $^{81}BrC_6H_4CO^+$), 183 (80, $^{79}BrC_6H_4CO^+$), 157 (19, [185 − CO]$^+$), 155 (20, [183 − CO]$^+$), 114 (4, $C_7H_8D_3O^+$), 104 (8), 97 (100, $C_7H_4D_3^+$).

The analogous data are displayed by *ent*-**8**.

5.2. cis-*Diols (+)- and (−)*-**5**. To a cooled soln. (*ca.* 0°) of **8** (2.91 g, 5.83 mmol) in anh. THF (50 ml), $LiAlH_4$ (445 mg, 11.7 mmol) was slowly added in portions and the mixture then kept at r.t. for 2 h (TLC monitoring). Extraction with Et_2O, workup, and CC (SiO_2, AcOEt) gave (+)-**5** (625 mg, 88%) as a colorless viscous oil that quickly solidified.

Starting from *ent*-**8** (2.88 g, 5.77 mmol) and $LiAlH_4$ (440 mg, 11.6 mmol), the analagous procedure afforded (−)-**5** (680 mg, 89%).

Data of (+)-**5**: White amorphous solid. M.p. 48–50°. R_f (AcOEt) 0.25. $[\alpha]_D^{25} = +31.9$ ($c = 1.00$, $CHCl_3$). IR (film): 3365*w*, 3324*s* (br.), 2923*s*, 2857*s*, 2661*m*, 2038*w*, 1445*s*, 1190*s*, 1093*s*, 1021*s*, 808*m*. ^{1}H-NMR (300 MHz, $CDCl_3$): 2.70 (CD_2OH); 2.59 (OH−C(2)); 1.82–1.73 (*m*, *dt*-like, H−C(1)); 1.70–1.23 (*m*, CH_2(3), CH_2(4), CH_2(5), CH_2(6)). ^{13}C-NMR (75.4 MHz, $CDCl_3$): 69.9 (*t*-like, $^1J(C,^2H) = 21.3$, C(2)); 66.2 (*quint.*-like, $^1J(C,^2H) = 21.7$, CD_2OH); 42.5 (C(1)); 32.9 (C(3)); 24.9 (C(6)); 23.6 (C(5)); 20.5 (C(4)). EI-MS: 133 (2, M^+, $C_7H_{11}D_3O_2^+$), 115 (25, [$M - H_2O]^+$), 97 (48, [$M - 2\,H_2O]^+$), 81 (30), 70 (100), 58 (60).

Data of (−)-**5**: $[\alpha]_D^{25} = -31.7$ ($c = 1.00$, $CHCl_3$). All other data: identical with those of (+)-**5**.

6. *Phosphorus Heterocycles* **9**–**12**. 6.1. *Phosphorus Reagents.* The 2,4-dinitrophenyl phosphorodichloridate was prepared according to [18]: $POCl_3$ (5 ml), anh. NaCl (7 mg), and 2,4-dinitrophenol were heated under reflux (*ca.* 120°) in a glove box under N_2 (48 h). After filtration and distilling off excess $POCl_3$, (bulb-to-bulb), the viscous residue crystallized (1.87 g, 92%). The product consisted of $Cl_2P(O)OC_6H_3(NO_2)_2$ (85%; ^{31}P-NMR ($CDCl_3$): 5.0) and $ClP(O)[OC_6H_3(NO_2)_2]_2$ (15%; ^{31}P-NMR($CDCl_3$): −6.5) and was not purified further.

$POCl_2F$ was prepared according to [19]: $POCl_3$ (100 g) and dry, finely crystalline NH_4F (48 g; *Fluka 09737, puriss. p.a.*) were heated at 110° (15 h) in a flask fitted with a condenser. The volatile fluorinated compounds passing through the condenser ($POCl_2F$ (b.p. 54°), $POClF_2$ (b.p. 3°), and POF_3 (b.p. −40°)) were trapped at −78°. The mixture from the cold trap was fractionally distilled (*Vigreux*, 50 cm) to afford $POCl_2F$ as a colorless liquid (11.6 g, 13%). B.p. 52°. ^{31}P-NMR ($CDCl_3$): 1.80 (*d*, $^1J(P,F) = 1191$).

6.2. trans- *and* cis-*3-(2,4-Dinitrophenoxy)-2,4-dioxa-3-phospha(1,5,5-$^2H_3$)bicyclo[4.4.0]decane 3-Oxides* ((+)- and (−)-**9a**, (+)- and (−)-**9b**, (+)- and (−)-**10a**, and (+) and (−)-**10b**, resp.). To a cooled soln. (0°) of (+)-**4** (50 mg, 0.38 mmol) and pyridine (60 µl) in anh. $CHCl_3$ (5 ml) in a glove box (N_2 atmosphere), a soln. (0°) of 2,4-dinitrophenyl phosphorodichloridate (145 mg, 0.48 mmol) in anh. $CHCl_3$ (2 ml) was added dropwise and the mixture kept at 0° for 2 h (TLC and GC/MS monitoring). The volatile components were evaporated and the residue subjected to CC (SiO_2, pH 5.6 [3], hexane/AcOEt 3:1 → 3:2): (+)-**9a** (38 mg, 28%) and (−)-**9b** (36 mg, 26%).

Applying the identical procedure, the following compounds were prepared from the different starting diols (each 50 mg): from (−)-**4**: (−)-**9a** (36 mg, 26%) and (+)-**9b** (40 mg, 29%); from (+)-**5**: (+)-

10a (61 mg, 45%), and (−)-**10b** (42 mg, 31%); from (−)-**5**: (−)-**10a** (65 mg, 47%) and (+)-**10b** (43 mg, 31%); in all cases the axial epimer was less polar.

*(+)-(1*S*,3*S*,6*R*)-3-(2,4-Dinitrophenoxy)-2,4-dioxa-3-phospha(1,5,5-$^2H_3$)bicyclo[4.4.0]decane 3-Oxide* ((+)-**9a**): Slightly yellowish prisms (from Et_2O/hexane). M.p. 125.5°. R_f (hexane/AcOEt 1:3) 0.57. $[\alpha]_D^{25} = +4.5$ ($c = 1.00$, $CHCl_3$). IR (KBr): 3271*m*, 3123*m*, 3065*w*, 2932*s*, 2864*s*, 2670*w*, 2508*w*, 2264*w*, 1916*w*, 1804*w*, 1613*s*, 1543*s*, 1453*m*, 1346*s*, 1261*s*, 1076*s*, 1022*s*, 934*s*, 899*s*, 835*s*, 782*s*, 661*m*, 607*m*, 485*s*. ^{1}H-NMR (300 MHz, $CDCl_3$): 8.83 (*dd*, $^4J(3',5') = 2.7$, $^5J(3',6') = 1.2$, H−C(3′)); 8.46 (*dd*, $^3J(5',6') = 9.2$, $^4J(5',3') = 2.7$, H−C(5′)); 8.13 (*dd*, $^3J(6',5') = 9.2$, $^5J(6',3') = 1.2$, H−C(6′)); 2.12 (*ddd*, $^3J = 12.5$, $^3J(10eq,9ax) = 3.4$, $^3J(10eq,9eq) = 2.0$, H_{eq}−C(10)); 2.05 (br. *d*, $^3J(6,7ax) = 11$, H−C(6))[22]; 1.94–1.80 (*m*, H_{eq}−C(9)); 1.84–1.70 (*m*, *tt*-like, H_{eq}−C(7), H_{eq}−C(8)); 1.59 (br. *td*, $^2J \approx {}^3J(10ax,9ax) \approx 11$, $^3J(10ax,9eq) = 3.5$, H_{ax}−C(10))[23]; 1.43–1.26 (*m*, *quint*.-like, H_{ax}−C(8), H_{ax}−C(9)); 1.07 (*qd*, $^2J \approx {}^3J(7ax,6) \approx {}^3J(7ax,8ax) \approx 12$, $^3J(7ax,8eq) = 3.5$, H_{ax}−C(7)). ^{13}C-NMR (75.4 MHz, $CDCl_3$): 148.2 (C(1′)); 143.4 (C(4′)); 140.6 (C(2′)); 129.2 (C(5′)); 123.0 (C(6′)); 121.9 (C(3′)); *ca.* 85 (*m*, C(1))[19]; *ca.* 74 (*m*, C(5))[19]; 40.7 (*d*, $^3J(6,P) = 6.4$, C(6)); 32.3 (*d*, $^3J(10,P) = 8.8$, C(10)); 25.2 (C(7)); 24.2 (C(8)); 23.9 (C(9)). ^{31}P-NMR (121.5 MHz, $CDCl_3$): −14.3 (*s*, $w_{1/2} \approx 10$, $^3J(P,^2H) \approx 3$)). EI-MS: 184 (100, $(NO_2)_2C_6H_3OH^+$), 154 (45), 107 (45), 91 (55), 79 (45), 63 (80), 53 (75). ESI-MS (MeOH/$CHCl_3$/NaI): 384 (100, $[M + Na]^+$, $[C_{13}H_{12}D_3N_2O_8P + Na]^+$).

*(−)-(1*R*,3*R*,6*S*)-3-(2,4-Dinitrophenoxy)-2,4-dioxa-3-phospha(1,5,5-$^2H_3$)bicyclo[4.4.0]decane 3-Oxide* ((−)-**9a**): $[\alpha]_D^{25} = -4.3$ ($c = 1.00$, $CHCl_3$). All other data: identical with those of (+)-**9a**.

*(+)-(1*R*,3*S*,6*S*)-3-(2,4-Dinitrophenoxy)-2,4-dioxa-3-phospha(1,5,5-$^2H_3$)bicyclo[4.4.0]decane 3-Oxide* ((+)-**9b**): Slightly yellowish needles (from Et_2O/hexane). M.p. 114°. R_f (hexane/AcOEt 1:3) 0.35. $[\alpha]_D^{25} = +46.9$ ($c = 1.00$, $CHCl_3$). IR (KBr): 3450*w*, 3116*m*, 3063*m*, 2939*s*, 2864*m*, 2544*w*, 2258*w*, 2175*w*, 2138*w*, 1936*w*, 1824*w*, 1613*s*, 1546*s*, 1487*s*, 1449*m*, 1417*m*, 1348*s*, 1314*s*, 1171*m*, 1149*m*, 1046*s*, 934*s*, 837*s*, 741*s*, 663*m*, 551*s*, 491*s*. ^{1}H-NMR (300 MHz, $CDCl_3$): 8.80 (*dd*, $^4J(3',5') = 2.7$, $^5J(3',6') = 1.2$, H−C(3′)); 8.45 (*dd*, $^3J(5',6') = 9.2$, $^4J(5',3') = 2.7$, H−C(5′)); 7.98 (*dd*, $^3J(6',5') = 9.2$, $^5J(6',3') = 1.2$, H−C(6′)); 2.33 (br. *d*, $^3J(6,7ax) = 11.5$, H−C(6))[22]; 2.20 (*dt*-like, $^2J = 12$, $^3J(10eq,9ax) \approx {}^3J(10eq,9eq) \approx 2$, H_{eq}−C(10)); 1.92–1.88 (*m*, H_{eq}−C(9)); 1.84–1.76 (*m*, H_{eq}−C(7), H_{eq}−C(8)); 1.57 (br. *td*, $^2J \approx {}^3J(10ax,9ax) \approx 12$, $^3J(10ax,9eq) = 3.5$, H_{ax}−C(10))[23]; 1.39–1.26 (*m*, *quint*.-like, H_{ax}−C(8), H_{ax}−C(9)); 1.03 (*qd*, $^2J \approx {}^3J(7ax,6) \approx {}^3J(7ax,8ax) \approx 12$, $^3J(7ax,8eq) = 3.5$, H_{ax}−C(7)). ^{13}C-NMR (75.4 MHz, $CDCl_3$)[20]: 148.3 (C(1′)); 143.6 (C(4′)); 140.3 (C(2′)); 128.9 (C(5′)); 123.9 (C(6′)); 121.5 (C(3′)); 38.9 (*d*, $^3J(6,P) = 12.4$, C(6)); 32.5 (*d*, $^3J(10,P) = 6.3$, C(10)); 26.3 (C(7)); 24.1 (C(8)); 23.8 (C(9)). ^{31}P-NMR (121.5 MHz, $CDCl_3$): −13.6 (*s*, $w_{1/2} \approx 8$, $^3J(P,^2H) \approx 2$)). EI-MS: 184 (100, $(NO_2)_2C_6H_3OH^+$), 154 (20), 107 (60), 91 (55), 79 (45), 63 (80), 53 (75). ESI-MS (MeOH/$CHCl_3$/NaI): 384 (100, $[M + Na]^+$, $[C_{13}H_{12}D_3N_2O_8P + Na]^+$).

*(−)-(1*S*,3*R*,6*R*)-3-(2,4-Dinitrophenoxy)-2,4-dioxa-3-phospha(1,5,5-$^2H_3$)bicyclo[4.4.0]decane 3-Oxide* ((−)-**9b**): $[\alpha]_D^{25} = -46.6$ ($c = 1.00$, $CHCl_3$). All other data: identical with those of (+)-**9a**.

*(+)-(1*S*,3*S*,6*S*)-3-(2,4-Dinitrophenoxy)-2,4-dioxa-3-phospha(1,5,5-$^2H_3$)bicyclo[4.4.0]decane 3-Oxide* ((+)-**10a**): Colorless viscous oil. R_f (hexane/AcOEt 1:3) 0.61. $[\alpha]_D^{25} = +36.8$ ($c = 1.00$, $CHCl_3$). IR ($CHCl_3$): 3114*w*, 3026*m*, 2945*s*, 2870*m*, 1609*s*, 1541*s*, 1485*m*, 1347*s*, 1317*s*, 1267*s*, 1224*m*, 1040*s*, 1013*s*, 934*s*, 899*s*, 867*w*, 668*s*, 612*m*, 553*m*, 453*m*. ^{1}H-NMR (300 MHz, $CDCl_3$): 8.81 (*dd*, $^4J(3',5') = 2.8$, $^5J(3',6') = 1.4$, H−C(3′)); 8.45 (*dd*, $^3J(5',6') = 9.0$, $^4J(5',3') = 2.8$, H−C(5′)); 7.98 (*dd*, $^3J(6',5') = 9.0$, $^5J(6',3') = 1.4$, H−C(6′)); 2.05 (*dd*, $^3J(6,7ax) = 12.0$, $^3J(6,7eq) = 4.0$, H−C(6)); 1.98–1.85 (*m*, H_{eq}−C(10)); 1.84–1.74 (*m*, H_{ax}−C(10)); 1.72–1.51 (*m*, $CH_2(7)$, $CH_2(9)$); 1.45–1.23 (*m*, $CH_2(8)$). ^{13}C-NMR (75.4 MHz, $CDCl_3$)[20]: 148.2 (C(1′)); 143.2 (C(4′)); 131.5 (C(2′)); 129.0 (C(3′)); 122.8 (C(5′)); 121.5 (C(6′)); 35.7 (*d*, $^3J(6,P) = 5.1$, C(6)); 31.0 (*d*, $^3J(10,P) = 9.2$, C(10)); 24.4 (C(7)); 22.9 (*d*, $^3J(8,P) = 16.0$, C(8)); 18.6 (*d*, $^3J(9,P) = 9.7$, C(9)). ^{31}P-NMR (121.5 MHz, $CDCl_3$): −14.4 (*s*, $w_{1/2} \approx 10$, $^3J(P,^2H) \approx 3$). ESI-MS (MeOH/$CHCl_3$/NaI): 384 (100, $[M + Na]^+$, $[C_{13}H_{12}D_3N_2O_8P + Na]^+$).

*(−)-(1*R*,3*R*,6*R*)-3-(2,4-Dinitrophenoxy)-2,4-dioxa-3-phospha(1,5,5-$^2H_3$)bicyclo[4.4.0]decane 3-Oxide* ((−)-**10a**): $[\alpha]_D^{25} = -35.1$ ($c = 1.00$, $CHCl_3$). All other data: identical with those of (+)-**10a**.

---

[22]) Line broadening due to $^3J(6ax,^2H_{ax}-C(5))$; $^3J(6ax,7eq)$ was not resolved.

[23]) Line broadening due to $^3J(10ax,^2H_{ax}-C(1))$.

*(+)-(1*R*,3*S*,6*R*)-3-(2,4-Dinitrophenoxy)-2,4-dioxa-3-phospha(1,5,5-$^2H_3$)bicyclo[4.4.0]decane 3-Oxide* ((+)-**10b**): Tiny colorless needles (from Et_2O/hexane). M.p. 158°. R_f (hexane/AcOEt 1:3) 0.41. $[\alpha]_D^{25} = +19.3$ ($c = 1.00$, $CHCl_3$). IR (KBr): 3120*w*, 3074*w*, 2936*m*, 2857*w*, 1610*s*, 1537*s*, 1483*w*, 1555*w*, 1342*s*, 1308*s*, 1255*m*, 1049*s*, 996*m*, 966*m*, 932*s*, 896*s*, 779*s*, 553*m*, 531*m*, 472*m*. ^{1}H-NMR (300 MHz, $CDCl_3$): 8.81 (*dd*, $^4J(3',5') = 2.8$, $^5J(3',6') = 1.4$, H–C(3′)); 8.45 (*dd*, $^3J(5',6') = 9.0$, $^4J(5',3') = 2.8$, H–C(5′)); 7.98 (*dd*, $^3J(6',5') = 9.0$, $^5J(6',3') = 1.4$, H–C(6′)); 2.36 (*t*, $^3J(6,7ax) \approx {}^3J(6,7eq) \approx 6$, H–C(6)); 2.19–2.04 (*m*, H_{eq}–C(10)); 1.90–1.72 (*m*, $CH_2(7)$, H_{ax}–C(10)); 1.70–1.58 (*m*, H_{eq}–C(9)); 1.44 (*m*, $w_{1/2} \approx 14$, $CH_2(8)$, H_{ax}–C(9)). ^{13}C-NMR (75.4 MHz, $CDCl_3$): 148.3 (C(1′)); 143.6 (C(4′)); 131.5 (C(2′)); 128.8 (C(3′)); 123.7 (C(5′)); 121.5 (C(6′)); *ca.* 82 (*m*, C(1)[19])[24]); 35.1 (*d*, $^3J(6,P) = 7.6$, C(6)); 29.0 (C(10)); 24.9 (C(7)); 22.2 (C(8)); 22.0 (C(9)). ^{31}P-NMR (121.5 MHz, $CDCl_3$): −13.8 (*s*, $w_{1/2} \approx 8$, $^3J(P,^2H) \approx 2$). EI-MS: 184 (100, $(NO_2)_2C_6H_3OH^+$), 154 (50), 94 (5), 91 (55), 79 (50), 53 (80). ESI-MS (MeOH/$CHCl_3$/NaI): 384 (100, $[M + Na]^+$, $[C_{13}H_{12}D_3N_2O_8P + Na]^+$).

*(−)-(1*S*,3*R*,6*S*)-3-(2,4-Dinitrophenoxy)-2,4-dioxa-3-phospha(1,5,5-$^2H_3$)bicyclo[4.4.0]decane 3-Oxide* ((−)-**10b**): $[\alpha]_D^{25} = -21.5$ ($c = 1.00$, $CHCl_3$). All other data: identical with those of (+)-**10b**.

6.3. trans- *and* cis-*3-Fluoro-2,4-dioxa-3-phospha(1,5,5-$^2H_3$)bicyclo[4.4.0]decane 3-Oxides* ((+)- and (−)-**11a**, (+)- and (−)-**11b**, (+)- and (−)-**12a**, and (+)- and (−)-**12b**, resp.). To a cooled soln. (0°) of (+)-**4** (80 mg, 0.60 mmol) in Et_2O (1 ml) in a glove box (N_2 atmosphere), anh. pyridine (97 µl (95 mg), 1.2 mmol) and a soln. of $POCl_2F$ (92 µl (137 mg), 1.0 mmol) in Et_2O (1 ml) were added with a syringe, and the mixture was kept for 5 min at 0° after which the mixture was withdrawn and quickly passed through SiO_2 (pH 5.6 [3], Et_2O). The precipitated pyridinium salt in the reaction flask was thoroughly washed with Et_2O, the combined soln. evaporated, and the residue subjected to CC (SiO_2 pH 5.6 [3], hexane/Et_2O 4:1) to yield (−)-**11a** (34 mg, 29%) and (−)-**11b** (37 mg, 31%).

Applying the identical procedure, the following compounds were prepared from the different starting diols (each 80 mg): from (−)-**4**: (+)-**11a** (38 mg, 32%) and (+)-**11b** (33 mg, 28%); from (+)-**5**: (+)-**12a** (39 mg, 33%) and (−)-**12b** (42 mg, 36%); from (−)-**5**: (−)-**12a** (41 mg, 35%) and (+)-**12b** (46 mg, 39%); in all cases the axial epimer was less polar.

*(+)-(1*R*,3*R*,6*S*)-3-Fluoro-2,4-dioxa-3-phospha(1,5,5-$^2H_3$)bicyclo[4.4.0]decane 3-Oxide* ((+)-**11a**): Colorless crystals (from Et_2O/hexane). M.p. 107°. R_f (hexane/Et_2O 1:3) 0.36. $[\alpha]_D^{25} = +14.0$ ($c = 1.00$, $CHCl_3$), $[\alpha]_D^{25} = +13.2$ ($c = 1.00$, acetone). IR (KBr): 3030*w*, 2946*s*, 2866*m*, 1474*w*, 1453*w*, 1331*s*, 1248*m*, 1066*s*, 996*s*, 900*s*, 885*s*, 626*m*. ^{1}H-NMR (300 MHz, $CDCl_3$): 2.14 (br. *d*, $^3J(6,7ax) = 11.6$, H–C(6))[22]); 1.98 (*dd*, $^2J = 20.5$, $^3J(10eq,9ax) = 8.5$, H_{eq}–C(10)); 1.93–1.83 (*m*, H_{eq}–C(9)); 1.79–1.69 (*m*, H_{eq}–C(7), H_{eq}–C(8)); 1.58 (br. *t*, $^2J \approx {}^3J(10ax,9ax) \approx 12$, H_{ax}–C(10))[25]); 1.41–1.18 (*m*, *quint.*-like, H_{ax}–C(8), H_{ax}–C(9)); 0.98 (*qd*, $^2J = {}^3J(7ax,6) = {}^3J(7ax,8ax) = 12.5$, $^3J(7ax,8eq) = 3.5$, H_{ax}–C(7)). ^{13}C-NMR (75.4 MHz, $CDCl_3$): *ca.* 84 (*m*, C(1))[19]); *ca.* 75 (*m*, C(5))[19]); 40.3 (*d*, $^3J(6,P) = 6.2$, C(6)); 32.1 (*d*, $^3J(10,P) = 9.2$, C(10)); 25.0 (C(7)); 24.0 (C(8)); 23.7 (*d*, $^4J(9,P) = 2.4$, C(9)). ^{31}P-NMR (121.5 MHz, $CDCl_3$): −15.4 (*d*, $^1J(P,F) = 1003$). ^{19}F-NMR (282.4 MHz, $CDCl_3$): −86.7 (*d*, $^1J(F,P) = 1003$). EI-MS: 197 (2, M^+, $C_7H_9D_3FO_3P^+$), 154 (7), 153 (5), 141 (2), 128 (1), 116 (3), 101 (12), 97 (90), 83 (26), 82 (82), 81 (100), 80 (89), 79 (23), 70 (23), 69 (19), 68 (25), 67 (17), 58 (18), 57 (16), 56 (22), 55 (28), 54 (23), 53 (17). CI-MS (NH_3): 409 (21, $[2M + NH_4]^+$), 215 (100, $[M + NH_4]^+$, $[C_7H_9D_3FO_3P + NH_4]^+$).

*(−)-(1*S*,3*S*,6*R*)-3-Fluoro-2,4-dioxa-3-phospha(1,5,5-$^2H_3$)bicyclo[4.4.0]decane 3-Oxide* ((−)-**11a**): $[\alpha]_D^{25} = -13.8$ ($c = 1.00$, $CHCl_3$), $[\alpha]_D^{25} = -12.9$ ($c = 1.00$, acetone). All other data: identical with those of (+)-**11a**.

*(+)-(1*R*,3*S*,6*S*)-3-Fluoro-2,4-dioxa-3-phospha(1,5,5-$^2H_3$)bicyclo[4.4.0]decane 3-Oxide* ((+)-**11b**): Colorless tiny needles (from Et_2O/hexane). M.p. 68°. R_f (hexane/Et_2O 1:3) 0.23. $[\alpha]_D^{25} = +26.5$ ($c = 1.00$, $CHCl_3$), $[\alpha]_D^{25} = +31.7$ ($c = 1.00$, acetone). IR (KBr): 3672*w*, 3480*w*, 3005*w*, 2870*m*, 1604*w*, 1475*w*, 1450*w*, 1325*s*, 1310*s*, 1090*m*, 1070*s*, 1055*m*, 1007*m*, 889*m*, 868*m*, 635*w*. ^{1}H-NMR (300 MHz, $CDCl_3$): 2.16 (*m*, *t*-like, H–C(6), H_{eq}–C(10)); 1.91 (*m*, *d*-like, $w_{1/2} \approx 20$, H_{eq}–C(9)); 1.81–1.71 (*m*, H_{eq}–C(7), H_{eq}–C(8)); 1.53 (br. *t*, $^2J \approx {}^3J(10ax,9ax) \approx 12$, H_{ax}–C(10))[25]); 1.41–1.22 (*m*, H_{ax}–C(8), H_{ax}–C(9)); 1.00 (*qd*, $^2J = {}^3J(7ax,6) \approx {}^3J(7ax,8ax) = 12.5$, $^3J(7ax,8eq) = 3.5$, H_{ax}–C(7)). ^{13}C-NMR (75.4 MHz, $CDCl_3$): *ca.* 84 (*m*, C(1))[19]); *ca.* 73 (*m*, C(5))[19]); 39.2 (*d*, $^3J(6,P) = 12.9$, C(6)); 32.4 (*d*, $^3J(10,P) = 6.3$, C(10)); 25.9

---

[24]) The signal of C(5) did not exceed the noise.

[25]) Line broadening due to $^3J(10ax,^2H_{ax}–C(1))$; $^3J(10ax,9eq)$ was not resolved.

(C(7)); 23.9 (C(8)); 23.6 (*d*, ^4J(9,P) = 1.9, C(9)). ^{31}P-NMR (121.5 MHz, $CDCl_3$): −14.9 (*d*, ^1J(P,F) = 992). ^{19}F-NMR (282.4 MHz, $CDCl_3$): −70.0 (*d*, ^1J(F,P) = 992)). ESI-MS: 197 (2, M^+, $C_7H_9D_3FO_3P^+$), 154 (9), 153 (7), 141 (3), 128 (2), 116 (4), 101 (15), 97 (89), 83 (26), 82 (85), 81 (100), 80 (89), 79 (26), 70 (24), 69 (22), 68 (26), 67 (17), 58 (20), 57 (17), 56 (23), 55 (28), 54 (24), 53 (16). CI-MS (NH_3): 409 (11, $[2M + NH_4]^+$), 215 (100, $[M + NH_4]^+$, $[C_7H_9D_3FO_3P + NH_4]^+$).

*(−)-(1*S*,3*R*,6*R*)-3-Fluoro-2,4-dioxa-3-phospha(1,5,5-$^2H_3$)bicyclo[4.4.0]decane 3-Oxide* ((−)-**11b**): $[\alpha]_D^{25} = -26.2$ (*c* = 1.00, $CHCl_3$), $[\alpha]_D^{25} = -32.2$ (*c* = 1.00, acetone). All other data: identical with those of (+)-**11b**.

*(+)-(1*S*,3*S*,6*S*)-3-Fluoro-2,4-dioxa-3-phospha(1,5,5-$^2H_3$)bicyclo[4.4.0]decane 3-Oxide* ((+)-**12a**): Colorless, viscous oil. R_f (hexane/Et_2O 1:3) 0.32. $[\alpha]_D^{25} = +21.4$ (*c* = 1.00, $CHCl_3$), $[\alpha]_D^{25} = +17.7$ (*c* = 1.00, acetone). IR ($CHCl_3$): 3033*w*, 2944*m*, 2871*w*, 1473*w*, 1444*m*, 1434*w*, 1371*w*, 1330*s*, 1093*s*, 1067*s*, 1014*s*, 985*s*, 959*m*, 899*s*, 847*m*. ^{1}H-NMR (300 MHz, $CDCl_3$): 2.08 (*dd*, ^3J(6,7ax) = 10.6, ^3J(6,7eq) = 2.5, H−C(6)); 1.96–1.83 (*m*, H_{eq}−C(9), H_{eq}−C(10)); 1.74 (*m*, *dt*-like, $w_{1/2} \approx 20$, H_{eq}−C(7)); 1.64–1.51 (*m*, CH_2(8), H_{ax}−C(9), H_{ax}−C(10)); 1.36 (*m*, *qd*-like, $w_{1/2} \approx 20$, H_{ax}−C(7)). ^{13}C-NMR (75.4 MHz, $CDCl_3$): *ca.* 81 (*m*, C(1))[19]; *ca.* 74 (*m*, C(5))[19]; 35.7 (*d*, ^3J(6,P) = 5.3, C(6)); 31.1 (*d*, ^3J(10,P) = 9.3, C(10)); 24.5 (C(7)); 22.8 (C(8)); 18.6 (C(9)). ^{31}P-NMR (121.5 MHz, $CDCl_3$): −15.5 (*d*, ^1J(P,F) = 1005). ^{19}F-NMR (282.4 MHz, $CDCl_3$): −86.4 (*d*, ^1J(F,P) = 1005)). EI-MS: 197 (1, M^+, $C_7H_9D_3FO_3P^+$), 154 (10), 153 (8), 141 (4), 128 (2), 116 (4), 101 (8), 97 (82), 83 (20), 82 (75), 81 (100), 80 (82), 79 (29), 70 (24), 69 (25), 68 (29), 67 (15), 58 (14), 57 (12), 56 (23), 55 (21), 54 (22), 53 (17). CI-MS (NH_3): 409 (100, $[2M + NH_4]^+$), 215 (100, $[M + NH_4]^+$, $[C_7H_9D_3FO_3P + NH_4]^+$).

*(−)-(1*R*,3*R*,6*R*)-3-Fluoro-2,4-dioxa-3-phospha(1,5,5-$^2H_3$)bicyclo[4.4.0]decane 3-Oxide* ((−)-**12a**): $[\alpha]_D^{25} = -21.2$ (*c* = 1.00, $CHCl_3$), $[\alpha]_D^{25} = -17.6$ (*c* = 1.00, acetone). All other data: identical with those of (+)-**12a**.

*(+)-(1*R*,3*S*,6*R*)-3-Fluoro-2,4-dioxa-3-phospha(1,5,5-$^2H_3$)bicyclo[4.4.0]decane 3-Oxide* ((+)-**12b**): Colorless, tiny prisms (from Et_2O/hexane). M.p. 62–64°. R_f (hexane/Et_2O 1:3) 0.22. $[\alpha]_D^{25} > 0$ (epimerization in $CHCl_3$), $[\alpha]_D^{25} = +7.9$ (*c* = 1.00, acetone). IR (KBr): 2950*m*, 2865*w*, 1480*w*, 1453*w*, 1339*m*, 1325*s*, 1150*m*, 1116*w*, 1089*m*, 1062*s*, 1018*m*, 1000*m*, 985*m*, 948*m*, 922*m*, 892*m*, 865*m*, 823*w*, 628*w*. ^{1}H-NMR (300 MHz, $(CD_3)_2CO$)[26]: 2.47 (*t*, ^3J(6,7ax) ≈ ^3J(6,7eq) ≈ 5, H−C(6)); 1.99–1.95 (*m*, CH_2(10)); 1.82–1.65 (*m*, CH_2(7), H_{eq}−C(9)); 1.50–1.40 (*m*, CH_2(8), H_{ax}−C(9)). ^{13}C-NMR (75.4 MHz, $(CD_3)_2CO$)[20]: 35.5 (*d*, ^3J(6,P) = 7.8, C(6)); 29.4 (C(10)); 25.4 (C(7)); 23.2 (C(8)); 22.4 (C(9)). ^{31}P-NMR (121.5 MHz, $(CD_3)_2CO$): −15.9 (*d*, ^1J(P,F) = 980). ^{19}F-NMR (282.4 MHz, $(CD_3)_2CO$): −77.1 (*d*, ^1J(F,P) = 980). EI-MS: 197 (1, M^+, $C_7H_9D_3FO_3P^+$), 154 (6), 153 (5), 140 (2), 128 (1), 116 (3), 102 (7), 101 (7), 97 (74), 83 (21), 82 (81), 81 (100), 80 (91), 79 (36), 70 (25), 69 (21), 68 (34), 67 (24), 58 (14), 57 (10), 56 (23), 55 (20), 54 (27), 53 (16). CI-MS (NH_3): 409 (100, $[2M + NH_4]^+$), 215 (100, $[M + NH_4]^+$, $[C_7H_9D_3FO_3P + NH_4]^+$).

*(−)-(1*S*,3*R*,6*S*)-3-Fluoro-2,4-dioxa-3-phospha(1,5,5-$^2H_3$)bicyclo[4.4.0]decane 3-Oxide* ((−)-**12b**): $[\alpha]_D^{25} < 0$ (epimerization in $CHCl_3$), $[\alpha]_D^{25} = -8.2$ (*c* = 1.00, acetone). All other data: identical with those of (+)-**12b**.

6.4. trans- *and* cis-N-*[(Benzyloxy)carbonyl]*-O-*(3-oxido-2,4-dioxa-3-phospha(1,5,5-$^2H_3$)bicyclo[4.4.0]dec-3-yl)*-L-*serine Methyl Esters* (**14a**/**14a′**, **14b**/**14b′**, **15a**/**15a′**, and **15b**/**15b′**). To a soln. of $POCl_3$ (273 µl (457 mg), 3.1 mmol) and pyridine (256 µl (251 mg), 3.17 mmol) in anh. Et_2O (6 ml) prepared at 0° in a glove box (N_2 atmosphere), a soln. containing (+)-*N*-[(benzyloxy)carbonyl]-L-serine methyl ester (805 mg, 3.17 mmol; *Bachem C-2605*) was added (*in situ* formation of **13**). After stirring for 2 h at 0°, (±)-**4** (400 mg, 3.0 mmol) and pyridine (485 µl (476 mg), 6.0 mmol) in anh. Et_2O (4 ml) were added, and the mixture was stirred for 12 h at r.t. and then evaporated. CC (SiO_2, $CHCl_3$/AcOEt 1:1) of the crude product (1.83 g) yielded the less polar axial epimers **14a**/**14a′** (205 mg, 16%) followed by the equatorial epimers **14b**/**14b′** (268 mg, 21%), both as a *ca.* 1:1 mixture of diastereoisomers.

The analogus procedure with (±)-**5** (400 mg, 3 mmol) in pyridine (256 µl (251 mg), 3.2 mmol), $POCl_3$ (273 µl (457 mg), 3.1 mmol), and (+)-*N*-[(benzyloxy)carbonyl]-L-serine methyl ester (806 mg, 3.17 mmol) furnished, after CC (SiO_2, Et_2O/MeOH 50:1) of the crude product (1.3 g), the *cis*-configurated diastereoisomers (each *ca.* 1:1) **15a**/**15a′** (260 mg, 20%) and **15b**/**15b′** (180 mg, 14%).

---

[26]) Due to epimerization in $CDCl_3$, the NMR spectra were recorded in $(CD_3)_2CO$.

N-*[(Benzyloxy)carbonyl]*-O-*[(1*RS,*3*RS,*6*SR)- *and* (*1*RS,*3*SR,*6*SR)-*3-oxido-2,4-dioxa-3-phospha(1,5,5-$^2H_3$)bicyclo[4.4.0]dec-3-yl]*-L-*serine Methyl Esters* (**14a**/**14a′** and **14b**/**14b′**, resp.). *Data of* **14a**/**14a′**: Colorless solid. M.p. 125–130°. R_f ($CHCl_3$/AcOEt 1:1) 0.31. ^{1}H-NMR (600 MHz, $CDCl_3$)[27]): 7.38–7.32 (*m*, *Ph*CH_2); 5.84 (br. *d*, ^3J(NH,2) = 7.7, NH); 5.15, 5.13 (*AB*, ^2J = 12.5, PhCH_2); 4.63 (*X* of *ABX*-P, br. *d*-like, $w_{1/2} \approx 15$, H–C(2)); 4.50 (*A* of *ABX*-P, *tq*-like, H_A–C(3)); 4.38 (*B* of *ABX*-P, *tt*-like, H_B–C(3)); 3.81 (*s*, MeO); 2.04 (*dt*, ^2J = 11.5, ^3J(10′eq,9′ax) ≈ ^3J(10′eq,9′eq) ≈ 2, H_{eq}–C(10′)); 1.87 (*m*, br. *t*-like, H–C(6′), H_{eq}–C(9′)); 1.73 (*m*, H_{eq}–C(8′)); 1.63 (*dq*, ^2J = 12, ^3J(7′eq,6′) ≈ ^3J(7′eq,8′ax) ≈ ^3J(7′eq,8′eq) ≈ 2, H_{eq}–C(7′)); 1.50 (*td*, $^2J \approx {}^3J$(10′ax,9′ax) ≈ 12, ^3J(10′ax,9′eq) = 3.5, H_{ax}–C(10′)); 1.31–1.23 (*m*, H_{ax}–C(8′), H_{ax}–C(9′)); 0.87 (br. *qd*, $^2J \approx {}^3J$(7′ax,6′) ≈ ^3J(7′ax,8′ax) ≈ 12, ^3J(7′ax,8′eq) ≈ 4, H_{ax}–C(7′)). ^{13}C-NMR (150.9 MHz, $CDCl_3$): 169.5 (C(1)); 155.7 (OCON); 136.0 (arom. C); 128.5 (2C), 128.2, 128.1 (2C) (arom. CH); 81.6 (*t*-like, ^3J(1′,P) ≈ ^1J(1′,^{2}H) ≈ 5, C(1′)); 71.5 (*quint.*-like, ^3J(5′,P) ≈ ^1J(5′,^{2}H) ≈ 5, C(5′)); 67.2 (Ph*C*H_2); 66.7, 66.6 (each *d*, ^2J(3,P) = 5.1, 4.9, C(3))[28]); 54.5 (*d*, ^3J(2,P) = 6.7, C(2)); 52.9 (MeO); 40.5 (*d*, ^3J(6′,P) = 5.9, C(6′)); 32.2 (*d*, ^3J(10′,P) = 9.1, C(10′)); 25.2 (C(7′)); 24.2 (C(8′)); 23.8 (C(9′)). ^{31}P{^{1}H}-NMR (242.9 MHz, $CDCl_3$): –6.66 (*t*-like, ^3J(P,^{2}H) = 3.5). ^{31}P{^{2}H}-NMR (242.9 MHz, $CDCl_3$): –6.66 (*t*, ^3J(P,H–C(3)) = 7.0). ^{31}P{^{1}H}-NMR (242.9 MHz, CD_3CN/D_2O/0.2M *Tris* (pH 7.8) 11:44:45): –5.12 (*s*, $w_{1/2} \approx 10$). ESI-MS (MeOH/$CHCl_3$/NaI): 453 (100, $[M + Na]^+$, $[C_{19}H_{23}D_3NO_8P + Na]^+$).

Data of **14b**/**14b′**: Slightly greenish viscous oil. R_f ($CHCl_3$/AcOEt 1:1) 0.16. ^{1}H-NMR (600 MHz, $CDCl_3$)[27]): 7.36–7.30 (*m*, *Ph*CH_2); 5.80 (*t*, ^3J(NH,2) ≈ ^4J(NH,3) ≈ 7.1, NH); 5.13 (*s*, PhCH_2); 4.57 (*X* of *ABX*-P, *dd*-like, $w_{1/2} \approx 15$, H–C(2)); 4.50 (*A* of *ABX*-P, *tt*-like, H_A–C(3)); 4.37 (*B* of *ABX*-P, *ddd*-like, H_B–C(3)); 3.77 (*s*, MeO); 2.04 (*m*, br. *dd*-like, H_{eq}–C(10′)); 1.89–1.80 (*m*, H–C(6′), H_{eq}–C(9′)); 1.72 (*m*, br. *d*-like, H_{eq}–C(8′)); 1.63 (*m*, *dq*-like, H_{eq}–C(7′)); 1.43 (*qd*-like, H_{ax}–C(10′)); 1.32–1.20 (*m*, *quint.*-like, H_{ax}–C(8′), H_{ax}–C(9′)); 0.92 (*m*, *qq*-like, H_{ax}–C(7′)). ^{13}C-NMR (150.9 MHz, $CDCl_3$): 169.2 (C(1)); 155.8 (OCON); 136.1 (arom. C); 128.5 (2C), 128.2, 128.1 (2C) (arom. CH); 81.6 (*t*-like, ^3J(1′,P) ≈ ^1J(1′,^{2}H) ≈ 5, C(1′)); 71.5 (*quint.*-like, ^3J(5′,P) ≈ ^1J(5′,^{2}H) ≈ 5, C(5′)); 67.8, 67.9 (each *d*, ^2J(3,P) = 5.5, 6.0, C(3))[28]); 67.1 (Ph*C*H_2); 54.3 (*d*, ^3J(2,P) = 6.6, C(2)); 52.8 (MeO); 40.5 (*d*, ^3J(6′,P) = 6.7, C(6′)); 32.4 (*d*, ^3J(10′,P) = 8.2, C(10′)); 25.5 (C(7′)); 24.3 (C(8′)); 23.8 (C(9′)). ^{31}P{^{1}H}-NMR (242.9 MHz, $CDCl_3$): –4.12 (*t*-like, ^3J(P,^{2}H) = 2.5). ^{31}P{^{2}H}-NMR (242.9 MHz, $CDCl_3$): –4.11, –4.13 (each *t*, ^3J(P,H–C(3)) = 6.5). ^{31}P{^{1}H}-NMR (242.9 MHz, CD_3CN/D_2O/0.2M *Tris* (pH 7.8) 11:44:45): –4.10 (*s*, $w_{1/2} \approx 10$). ESI-MS (MeOH/$CHCl_3$/NaI): 453 (100, $[M + Na]^+$, $[C_{19}H_{23}D_3NO_8P + Na]^+$).

N-*[(Benzyloxy)carbonyl]*-O-*[(1*RS,*3*RS,*6*SR)- *and* (*1*RS,*3*SR,*6*RS)-*3-oxido-2,4-dioxa-3-phospha(1,5,5-$^2H_3$)bicyclo[4.4.0]dec-3-yl]*-L-*serine Methyl Esters* (**15a**/**15a′** and **15b**/**15b′**, resp.). *Data of* **15a**/**15a′**: Colorless solid. M.p. 81–84°. R_f ($CHCl_3$/AcOEt 1:1) 0.32, R_f (Et_2O/MeOH 50:1) 0.16. ^{1}H-NMR (600 MHz, $CDCl_3$)[27]): 7.29–7.25 (*m*, *Ph*CH_2); 5.82 (br. *d*, ^3J(NH,2) = 7.7, NH); 5.07, 5.05 (*AB*, ^2J = 13, PhCH_2); 4.53 (*X* of *ABX*-P, br. *dd*-like, $w_{1/2} \approx 18$, H–C(2)); 4.39 (*A* of *ABX*-P, *td*-like, H_A–C(3)); 4.30 (*B* of *ABX*-P, br. *t*-like, $w_{1/2} \approx 20$, H_B–C(3)); 3.72 (*s*, MeO); 1.87 (br. *td*-like, $^2J \approx 13$, $^2J \approx 3$, H_{eq}–C(9′), H_{eq}–C(10′)); 1.74 (br. *d*-like, $^2J \approx 13$, H–C(6′)); 1.57–1.38 (*m*, not resolved, H_{eq}–C(7′), CH_2(8′), H_{ax}–C(9′), H_{ax}–C(10′)); 1.21 (*qt*-like, $^2J \approx {}^3J$(7′ax,6′) ≈ ^3J(7′ax,8′ax) ≈ 13, ^3J(7′ax,8′eq) ≈ 4, H_{ax}–C(7′)). ^{13}C-NMR (150.9 MHz, $CDCl_3$): 169.5 (C(1)); 155.7 (OCON); 136.0 (arom. C); 128.4 (2C), 128.1, 128.0 (2C) (arom. CH); *ca.* 78 (*m*, C(1′))[19]); *ca.* 73 (*m*, C(5′))[19]); 67.1 (Ph*C*H_2); 66.7, 66.5 (each *d*, ^2J(3,P) = 4.3, 4.2, C(3))[28]); 54.4 (*d*, ^3J(2,P) = 5.8, C(2)); 52.8 (MeO); 35.7 (*d*, ^3J(6′,P) = 5.1, C(6′)); 31.1 (*d*, ^3J(10′,P) = 8.6, C(10′)); 24.5 (C(7′)); 22.8 (C(8′)); 18.6 (C(9′)). ^{31}P{^{1}H}-NMR (242.9 MHz, $CDCl_3$): –6.49 (*s*-like, $w_{1/2} \approx 8$). ^{31}P{^{2}H}-NMR (242.9 MHz, $CDCl_3$): –6.49 (*m*, $w_{1/2} \approx 22$). ^{31}P{^{1}H}-NMR (161.9 MHz, CD_3CN/D_2O/0.2M *Tris* (pH 7.8) 11:44:45): –5.38 (*t*-like, $w_{1/2} \approx 10$). ESI-MS (CH_2Cl_2/MeCN/NaI): 453 (100, $[M + Na]^+$, $[C_{19}H_{23}D_3NO_8P + Na]^+$).

---

[27]) The diastereoisomerism of these mixtures was significantly revealed in the ^{1}H-NMR at 600 MHz as compared to that at 300 MHz. Most of the signals were doubled but the individual lines were overlapping, a fact that resulted in an overall lower resolution compared to spectra at 300 MHz. A full interpretation of the data is only made in those cases where the coupling situation was unambiguous.

[28]) Double signals due to diastereoisomerism.

Data of **15b**/**15b′**: Colorless viscous oil. R_f ($CHCl_3$/AcOEt 1:1) 0.16, R_f (Et_2O/MeOH 50:1) 0.05. ^{1}H-NMR (600 MHz, $CDCl_3$)[27]): 7.29–7.21 (*m*, *Ph*CH_2); 5.82 (br. *d*, ^3J(NH,2) = 7.5, NH); 5.06 (*s*, PhCH_2); 4.52 (*X* of *ABX*-P, br. *dt*-like, $w_{1/2} \approx 16$, H–C(2)); 4.46 (*A* of *ABX*-P, *tt*-like, H_A–C(3)); 4.33 (*B* of *ABX*-P, *ddd*-like, H_B–C(3)); 3.71 (*s*, MeO); 2.09–1.14 (*m*, not resolved, H–C(6′), CH_2(7′), CH_2(8′), CH_2(9′), CH_2(10′)). ^{13}C-NMR (150.9 MHz, $CDCl_3$): 169.1 (C(1)); 155.7 (OCON); 136.0 (arom. C); 128.4 (2C), 128.1, 127.9 (2C) (arom. CH); *ca.* 77 (*m*, C(1′))[19]); *ca.* 71 (*m*, C(5′))[19]); 67.9 (*d*, ^2J(3,P) = 5.3, C(3)); 67.0 (PhCH_2); 54.4 (*d*, ^3J(2,P) = 5.8, C(2)); 52.8 (MeO); 35.5 (*d*, ^3J(6′,P) = 5.1, C(6′)); 30.3 (*d*, ^3J(10′,P) = 7.1, C(10′)); 23.9 (C(7′)); 23.7 (C(8′)); 19.9 (C(9′)). ^{31}P{^{1}H}-NMR (242,9 MHz, $CDCl_3$): –3.93 (*s*-like, $w_{1/2} \approx 8$). ^{31}P{^{2}H}-NMR (242.9 MHz, $CDCl_3$): –3.93 (*m*, $w_{1/2} \approx 20$). ^{31}P{^{1}H}-NMR (242.9 MHz, CD_3CN/D_2O/0.2M *Tris* (pH 7.8) 11:44:45): –3.77, –3.95 (each *s*, $w_{1/2} \approx 10$). ESI-MS (CH_2Cl_2/MeCN/NaI): 453 (100, $[M+Na]^+$, $[C_{19}H_{23}D_3NO_8P+Na]^+$).

7. *2D ^{31}P-NMR Experiments with δ-Chymotrypsin. Sample Preparation.* The freshly prepared soln. of one of the enantiomerically pure inhibitors **9**–**12** (0.6 mg, 1.65 μmol) in CD_3CN (60 μl) was quickly added to a freshly prepared soln. of δ-chymotrypsin (40 mg, 1.6 μmol) in D_2O (240 μl)/*Tris* buffer (250 μl; pH 7.8, 0.2M) and mixed in a *Vortex*®. The mixture (yellow with the 2,4-dinitrophenoxy substituted inhibitors **9** and **10** due to partial hydrolysis) was transferred into an NMR tube (5 mm i.d.) and kept for 2 d at r.t. in the dark[29]).

NMR Parameters. General: Bruker DRX-600 spectrometer, 242.9 MHz, T 300 ± 1 K; δ(^{31}P) in ppm rel. to 85% H_3PO_4 (= 0 ppm) as external reference; window function in F_1 and F_2 = sine 2; 1000 transients. 2D H-1/X Correlation *via* heteronuclear zero and double quantum coherence; phase sensitive using TPPI with decoupling during acquisition; peak type selection by using gradient pulses with coherence selection step after t_1.

Inhibition Experiments with the 2,4-Dinitrophenoxy-Substituted Inhibitors **9** *and* **10**: Relaxation delay 1.5 s; acquisition time 0.213 s; spectral widths 1440 Hz (2.4 ppm (F_1, ^{1}H)), 1950 Hz (8.0 ppm (F_2,^{31}P)); time domain in F_1 = 31.

Inhibition Experiments with the Fluoro-Substituted Inhibitors **11** and **12**: Relaxation delay 1.5 s; acquisition time 0.1316 s; spectral widths 6600 Hz (11.0 ppm (F_1, ^{1}H)), 1950 Hz (8.0 ppm, (F_2,^{31}P)); time domain in F_1 = 2048.

REFERENCES

[1] W. Ganci, E. J. M. Meier, F. Merckling, G. Przibille, U. Ringeisen, P. Rüedi, *Helv. Chim. Acta* **1997**, *80*, 421.

[2] S. Furegati, W. Ganci, G. Przibille, P. Rüedi, *Helv. Chim. Acta* **1998**, *81*, 1127.

[3] S. Furegati, W. Ganci, F. Gorla, U. Ringeisen, P. Rüedi, *Helv. Chim. Acta* **2004**, *87*, 2629.

[4] S. Furegati, M. Binder, A. Linden, P. Rüedi, *Helv. Chim. Acta* **2006**, *89*, 1351, and refs. cit. therein.

[5] M. J. Stöckli, P. Rüedi, *Helv. Chim. Acta* **2001**, *84*, 106.

[6] J. Sanchez Real, J. Pascual, *An. Fis. Quim., B* **1953**, *49*, 445; M. A. Febrer, P. Gomis, J. Pascual, *An. Fis. Quim.* **1964**, *60*, 671; P. Gomis Torne, *Rev. Real. Acad. Cienc. Exactas, Fis. Natur. Madrid* **1966**, *60*, 419; K. Chilina, U. Thomas, A. F. Tucci, K. D. Michael, C. M. Stevens, *Biochemistry* **1969**, *8*, 2846; R. U. Lemieux, J. T. Brewer, *Adv. Chem. Ser.* **1973**, *117*, 121.

[7] G. Przibille, Internal Progress Reports, University of Zurich, 1995, 1996; S. Furegati, A. Linden, G. Przibille, D. Rentsch, P. Rüedi, '1st Electronic Conference on Synthetic Organic Chemistry' (ECSOC-1), 1–30 September 1997; http://unibas.ch/mdpi/ecsoc/a0034/a0034.htm.

[8] M. Wächter, 'Herstellung optisch aktiver Organophosphate mit *cis*- und *trans*-Decalingerüst zur Untersuchung der Inhibition von Acetylcholinesterase', M. Sc. Thesis, University of Zurich, 2005.

[9] N. K. Schaffer, C. S. May, W. H. Summerson, *J. Biol. Chem.* **1953**, *202*, 67; D. M. Blow, J. J. Birktoft, B. S. Hartley, *Nature* **1969**, *221*, 337; D. M. Blow, *Acc. Chem. Res.* **1976**, *9*, 145; J. Kraut, *Annu. Rev. Biochem*. **1977**, *46*, 33; P. A. Frei, S. A. Whitt, J. B. Tobin, *Science* **1981**, *264*, 1927; T. A. Steitz, R. G.

---

[29]) Due to turbidity of the sample, no NMR spectra could be recorded when the soln. was kept at lower temperature.

Shulman, *Annu. Rev. Biophys. Bioeng*. **1982**, *11*, 419; L. Polgar, in 'Hydrolytic Enzymes', Eds. A. Neuenberger and K. Brocklehurst, Elsevier, Amsterdam, 1987.
[10] F. Merckling, P. Rüedi, *Tetrahedron Lett.* **1996**, *37*, 2217.
[11] G. R. J. Thatcher, R. Kluger, *Adv. Phys. Org. Chem.* **1989**, *25*, 99.
[12] F. H. Westheimer, *Acc. Chem. Res.* **1968**, *1*, 70; R. F. Hudson, C. Brown, *Acc. Chem. Res.* **1972**, *5*, 204; P. Gillespie, F. Ramirez, I. Ugi, D. Marquarding, *Angew. Chem., Int. Ed.* **1973**, *12*, 109; S. Tripett, *Pure Appl. Chem.* **1974**, *40*, 595.
[13] F. Eckstein, P. J. Romaniuk, B. A. Connolly, *Methods Enzymol.* **1982**, *87*, 197; S. A. Buchwald, D. E. Hansen, A. Hassett, J. R. Knowles, *Methods Enzymol.* **1982**, *87*, 279; G. Lowe, *Acc. Chem. Res.* **1983**, *16*, 244.
[14] R. Wolfenden, *Acc. Chem. Res.* **1972**, *5*, 10; G. E. Lienhard, *Science* **1973**, *180*, 149; R. Huber, W. Bode, *Acc. Chem. Res.* **1978**, *11*, 114; A. Warshel, G. Naray-Szabo, F. Sussman, J. K. Hwang, *Biochemistry* **1989**, *28*, 3629.
[15] N. S. Sampson, P. A. Bartlett, *Biochemistry* **1991**, *30*, 2255; R. Bone, N. S. Sampson, P. A. Bartlett, D. A. Agard, *Biochemistry* **1991**, *30*, 2263.
[16] C. M. Thomson, S. Ryu, C. E. Berkman, *J. Am. Chem. Soc.* **1992**, *114*, 10710.
[17] R. F. Toia, J. E. Casida, *Biochem. Pharmacol.* **1979**, *28*, 3307; A. C. M. van der Drift, H. C. Beck, W. H. Dekker, A. G. Hulst, E. R. J. Wils, *Biochemistry* **1985**, *24*, 6894; J. Grunwald, Y. Segall, E. Shirin, D. Waysbort, N. Steinberg, I. Silman, Y. Ashani, *Biochem. Pharmacol.* **1989**, *38*, 3157.
[18] C. A. Bunton, E. J. Fendler, J. H. Fendler, *J. Am. Chem. Soc.* **1967**, *89*, 1221.
[19] C. J. Wilkins, *J. Chem. Soc.* **1951**, 2726.

Received July 2, 2007